

**UCSF**

**UC San Francisco Electronic Theses and Dissertations**

**Title**

Ablation and caries inhibition of pits and fissures using CO<sub>2</sub>, Er:YAG, and Er:YSGG laser irradiation

**Permalink**

<https://escholarship.org/uc/item/7qj1390v>

**Author**

Young, Douglas A.

**Publication Date**

2000

Peer reviewed|Thesis/dissertation

**ABLATION AND CARIES INHIBITION OF PITS AND FISSURES  
USING CO<sub>2</sub>, Er:YAG, AND Er:YSGG LASER IRRADIATION**

by

**DOUGLAS A. YOUNG**

**THESIS**

Submitted in partial satisfaction of the requirements for the degree of

**MASTER OF SCIENCE**

in

**Oral Biology**

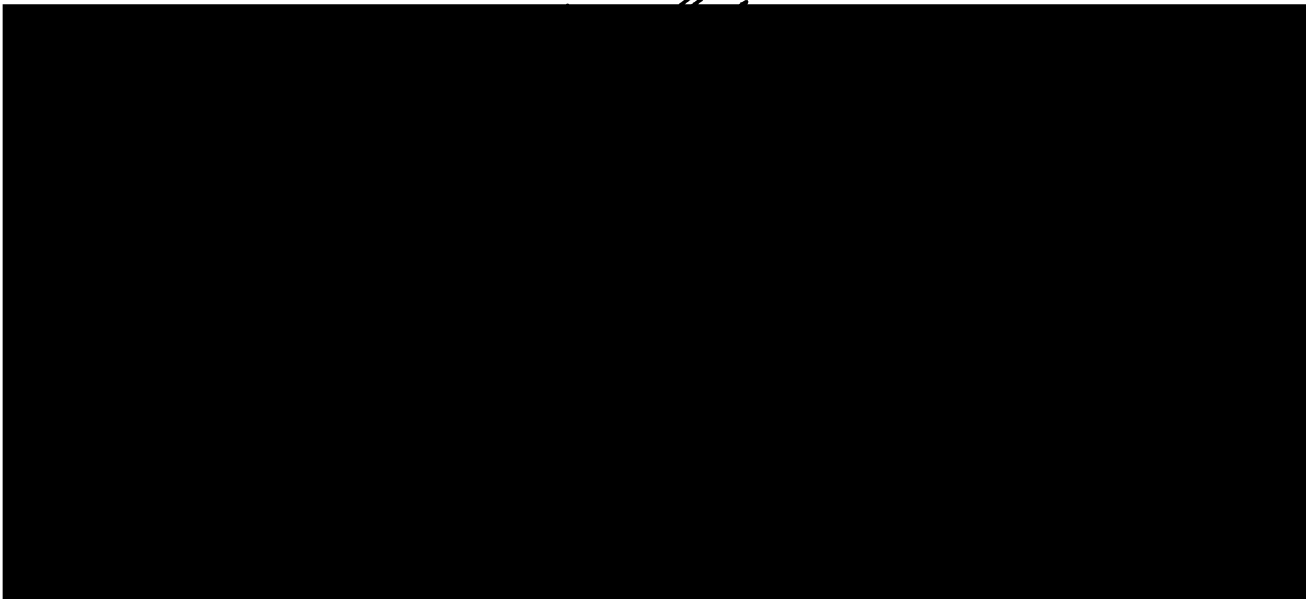
in the

**GRADUATE DIVISION**

of the

**UNIVERSITY OF CALIFORNIA**

**San Francisco**



## **ACKNOWLEDGMENTS**

Several years ago I committed myself to gain knowledge in Cariology. For this I went to the one of the world's most renown leaders in the field, John Featherstone. This special individual inspired me so much that I decided to obtain my Masters in Oral Biology and continue research in this field. It is because of his careful guidance, not only as my research mentor but also as a person whom I hold in the highest regard, that I was able to accomplish my goal and for this I must express my deepest gratitude and appreciation.

I would like to also thank Dan Fried who guided me on the technical aspects of this project and also served on my thesis committee, as did Art Miller. Their advise and hard work is greatly appreciated.

I wish to express my gratitude to the following individuals in the lab that made me feel welcome and helped me get accustomed to new procedures and equipment: Marcia Rapozo-Hilo, Cliff Duhn, and Eric Zaremski. Last but not least, I wish to thank to all those that encouraged me throughout the program including my principal advisor John Greenspan, Peter Jacobsen, Alan Budenz and, of course, my family. I could not have done it without your encouragement and support.

## **ABSTRACT**

Pit and fissure caries remain the most common form of caries and are difficult to detect and prevent. In this study, the hypothesis that specific infrared (IR) laser irradiation used for ablation of the occlusal pits and fissures can also inhibit caries progression was tested. To complete this study on the pits and fissures, higher fluences were used to test this hypothesis than were used by previous studies. Occlusal pits and fissures of extracted human teeth were ablated with Er:YAG ( $\lambda=2.94 \mu\text{m}$ , 200  $\mu\text{s}$  pulse duration, 64 J/cm<sup>2</sup> incident fluence), Er:YSGG ( $\lambda=2.79 \mu\text{m}$ , 200  $\mu\text{s}$  pd, 105 J/cm<sup>2</sup> if) or CO<sub>2</sub> ( $\lambda=9.6 \mu\text{m}$ , 5  $\mu\text{s}$  pd, 6.1 J/cm<sup>2</sup> if) laser irradiation (n=10 per group). "Enamelplasty" performed on non-irradiated pits and fissures using a high-speed 1/4 round carbide bur served as the control group. After laser ablation in the test groups and enamelplasty in the control group, artificial caries-like lesions were created by subjecting the teeth to pH cycling. Thin (80  $\mu\text{m}$ ) sections were then analyzed utilizing polarized light microscopy and transverse microradiography (TMR). The mean relative mineral loss, or  $\Delta Z$  values, measured in vol. %  $\times \mu\text{m}$  and (standard deviations) were 2074(929) for bur control, 1053(787) for Er:YAG, 583(261) for Er:YSGG, and 1047(416) for the CO<sub>2</sub> group. Laser ablation of the pits and fissures resulted in a 50% inhibition of caries progression for both CO<sub>2</sub> and Er:YAG, and 72% caries inhibition for Er:YSGG. All laser groups were significantly superior in caries inhibition at a statistical level of  $p<0.01$  compared to the control (bur) group, however there was no significant difference between the three lasers groups. Results indicate that these lasers can not only conservatively prepare pits and fissures but, in addition, can have significant preventive effects against caries. In addition, the high fluence levels used in this study did not seem to demonstrate any adverse effects on caries inhibition.

## **TABLE OF CONTENTS**

	<b>Page</b>
<b>TITLE PAGE</b>	<b>i</b>
<b>ACKNOWLEDGMENTS</b>	<b>ii</b>
<b>ABSTRACT</b>	<b>iii</b>
<b>TABLE OF CONTENTS</b>	<b>iv</b>
<b>LIST OF FIGURES</b>	<b>vii</b>
<b>LIST OF TABLES</b>	<b>ix</b>
<b>A. BACKGROUND AND SPECIFIC AIM</b>	
<b>A.1 INTRODUCTION</b>	<b>1</b>
A.1.1. Hypothesis to be tested	<b>3</b>
<b>A.2 LITERATURE REVIEW</b>	<b>3</b>
A.2.1 Proposed laser systems for caries inhibition	<b>3</b>
A.2.1.1 Relevant laser physics	<b>4</b>
A.2.1.2 Hard tissue optics	<b>6</b>
A.2.1.3 Wavelength	<b>7</b>
A.2.1.4 Pulse duration	<b>9</b>
A.2.1.5 Pulse energy and fluence	<b>9</b>
A.2.1.6 Repetition rate and number of pulses	<b>10</b>
A.2.1.7 Proposed mechanism of caries inhibition	<b>10</b>
A.2.1.8 Ablation mechanisms	<b>11</b>
A.2.1.9 Surface temperatures and residual energy	<b>12</b>
A.2.1.10 Peripheral thermal damage	<b>13</b>

A2.2 The caries process	13
A2.2.1 Demineralization	14
A2.2.2 Conventional management of the occlusal surface	15
A2.2.3 Caries Management by Risk Assessment (CAMBRA)	16
A.3 SPECIFIC AIM	17
<b>B. EXPERIMENTAL DESIGN AND METHODS</b>	
B.1. SAMPLE PREPARATION AND LASER ABLATION	18
B.1.1 Sample selection and preparation	18
B.1.2 CO <sub>2</sub> , Er:YAG, and Er:YSGG laser ablation	20
B.1.3 Preparation of remineralization and demineralization solutions and their analysis	24
B.1.3.1 Calcium analysis using atomic absorption (AA) spectrophotometer	25
B.1.3.2 Phosphate analysis using UV spectrophotometer	25
B.1.3.3 pH calibration	26
B.1.4 Creating <i>in vitro</i> decalcification	26
B.1.5 Preparation of thin sections using the hard tissue microtome	27
B.1.6 Polarized light microscopy	28
B.1.7 Transverse Microradiography (TMR)	29
B.1.8 Statistical analysis	30
B.1.8.1 Deficiencies and errors	30

UCSF LIBRARY

<b>C. RESULTS</b>	
C.1 RELATIVE MINERAL LOSS ( $\Delta Z$ ) AND PERCENT INHIBITION	32
C.2 DATA ANALYSIS	34
C.3 POLARIZED LIGHT MICROSCOPY (PLM)	35
C.4 TRANSVERSE MICRORADIOGRAPHY (TMR)	36
<b>D. DISCUSSION</b>	38
<b>E. REFERENCES</b>	44
<b>F. APPENDIX</b>	
F.1 APPENDIX A: FLUENCE CALCULATIONS	50
F.2 APPENDIX B: STATISTICAL CALCULATIONS (ANOVA)	51
F.3 APPENDIX C: STATISTICAL CALCULATIONS (SNK)	52

UCSF LIBRARY

## LIST OF FIGURES

		<b>Page</b>
<b>Figure 1</b>	IR transmission spectrum of carbonated hydroxyapatite (<1%) in a compacted KBr pellet.	8
<b>Figure 2</b>	Diagram of the occlusal experimental scheme.	19
<b>Figure 3</b>	Er:YAG laser beam profile	21
<b>Figure 4</b>	Er:YSGG laser beam profile	22
<b>Figure 5</b>	CO <sub>2</sub> laser beam profile	22
<b>Figure 6</b>	Diagram showing the direction of the saw cuts in relation to the laser and bur cuts.	28
<b>Figure 7</b>	Polarized light microscopy of YSGG laser treated samples	35
<b>Figure 8</b>	Polarized light microscopy of CO <sub>2</sub> laser treated samples	35
<b>Figure 9</b>	Polarized light microscopy of YAG laser treated samples	35



<b>Figure 10</b>	Polarized light microscopy of bur control treated samples	35
<b>Figure 11</b>	Transverse microradiography of YSGG laser treated samples	36
<b>Figure 12</b>	Transverse microradiography of CO <sub>2</sub> laser treated samples	36
<b>Figure 13</b>	Transverse microradiography of YAG laser treated samples	37
<b>Figure 14</b>	Transverse microradiography of bur control treated samples	37

UCSF LIBRARY

## LIST OF TABLES

		Page
<b>Table 1</b>	Summary of laser parameters used in the present study	23
<b>Table 2</b>	Summary of the solution analysis	26
<b>Table 3</b>	Summary of results for listed laser parameters	32
<b>Table 4</b>	Mineral Loss [Vol% um], mean, SD and % inhibition for each sample	33

UCSF LIBRARY

## **A. BACKGROUND AND SPECIFIC AIMS**

### **A.1 Introduction**

Previous studies using an *in vitro* pH cycling model have shown that CO<sub>2</sub> laser irradiation ( $\lambda=9-11 \mu\text{m}$ ) can be used specifically to treat dental enamel surfaces and inhibit the progression of caries-like lesions as high as 85%[1-3]. This is a similar inhibition level to that achieved by daily application of a sodium fluoride-containing dentifrice (70-85%)[4]. However, in these previous studies, the CO<sub>2</sub> laser used was not suitable for ablation of enamel. A subsequent study showed that Er:YAG ( $\lambda=2.94 \mu\text{m}$ ) and Er:YSGG ( $\lambda=2.79 \mu\text{m}$ ) lasers used specifically to ablate dental enamel on smooth surfaces could also exhibit caries inhibition of 40% and 60% respectively[5] in the same *in vitro* model.

Dental enamel is 85% by volume carbonated hydroxyapatite which comprises the mineral component. The remaining 15% by volume is comprised of lipids, protein, and water and represents the diffusion channels through which small molecules such as acids may diffuse into the enamel thus causing demineralization of tooth mineral[6, 7]. The enamel contains between 2-5% carbonate in the mineral, which represents enamel defects or imperfections in the enamel crystals that are preferentially attacked by the acid during an acid challenge[8]. Previous studies have proposed that heating the enamel surface temperature to ranges of 400-1200°C will cause elimination of the carbonate and make the surface resistant to acid dissolution[1-3, 9-11].

The clinical implication of the present study is the possibility that the Er:YSGG, Er:YAG, and perhaps the CO<sub>2</sub> laser could be used for both ablation and caries preventive treatment of dental hard tissues. Clinically, this would be especially significant in the pit and fissure sites since historically they have been a difficult area for the clinical dentist to

UCSF LIBRARY

effectively prevent or conservatively treat dental caries. The narrow morphology of the pits and fissures causes several problems. First, these are the perfect niches for pathogenic caries organisms to proliferate[12], and they are not cleansible by traditional means, thus making them highly cariogenic sites. Second, it is difficult to detect caries in these areas[13] and the use of a sharp dental explorer has been ineffective and 60% inaccurate[14]. Lastly, it is difficult to deliver fluoride to pits and fissures. Currently, it is impossible to clinically monitor the effectiveness of remineralization. Traditional methods utilizing "extension for prevention" as first described by G.V. Black often result in removing unnecessary tooth structure and is no longer well supported by current research in the field[15, 16]. Modern caries management combines chemical treatment of dental caries with advances in dental materials and conservative restorative techniques, and is rapidly becoming more popular[16-18]. Recently, advances in laser dentistry have made it potentially possible to ablate enamel, assist in preventing caries and to micromechanically "etch" the surface for bonding, all in one procedure. If this is true, utilization of dental lasers in this fashion prior to placement of sealants, preventive resin restorations or other bonded restorative materials not only will accomplish multiple tasks, but also would provide a caries resistant surface in an area difficult to deliver fluoride and would be a significant contribution to contemporary treatment of dental caries. Therefore, it is quite possible that a single laser could be used to conservatively remove debris or caries, adequately etch[19, 20] the enamel surface for bonding procedures, and preventively inhibit future caries simultaneously, and thus may be preferable over a dental handpiece in the pit and fissure areas where fluoride delivery is problematic.

The objective of this study was to evaluate the susceptibility of dental enamel to acid dissolution using an artificial caries-like lesion model after the pit and fissure areas on

extracted human teeth were ablated with CO<sub>2</sub>, Er:YAG, or Er:YSGG laser irradiation. It may be possible to utilize one or more of these laser conditions clinically to achieve ablation, micromechanical surface preparation, and caries prevention.

#### **A.1.1. Hypothesis to be tested**

The hypothesis to be tested in this study was that CO<sub>2</sub> ( $\lambda=9.6 \mu\text{m}$ ), Er:YAG ( $\lambda=2.94 \mu\text{m}$ ) and Er:YSGG ( $\lambda=2.79 \mu\text{m}$ ) laser irradiation used specifically to ablate the pits and fissures will exhibit caries inhibition effects.

### **A.2 Literature Review**

#### **A.2.1 Proposed laser systems for caries inhibition and ablation**

Traditionally, CO<sub>2</sub> laser systems are very commonly used for soft tissue surgery of the oral mucous membranes. These lasers operate at 10.6  $\mu\text{m}$  in continuous wave mode. The first work using CO<sub>2</sub> laser systems for caries preventive treatments on dental hard tissues was done by Stern in the 1960's using continuous wave CO<sub>2</sub> lasers ( $\lambda=10.6 \mu\text{m}$ ), with very disappointing results[21, 22]. The peripheral heat deposition in the tooth caused unacceptable peripheral thermal damage[23]. This problem was solved by the use of pulsed laser systems. In 1986, the use of 9.3  $\mu\text{m}$  and 9.6  $\mu\text{m}$  wavelengths were shown to be more efficient for caries preventive effects[24]. It was later discovered that pulsed CO<sub>2</sub> lasers could also effectively ablate dental hard tissue[25]. The absorption coefficient of enamel at  $\lambda=9.6 \mu\text{m}$  is approximately 10 times higher than the conventional 10.6  $\mu\text{m}$  CO<sub>2</sub> wavelength. The success of the CO<sub>2</sub> lasers at these wavelengths was attributed to this high absorption by tooth mineral as will be discussed in detail below.

UCSF LIBRARY

Recently, there has been much interest in using lasers to cut or ablate tooth structure for cavity preparation. Two laser systems, the Er:YAG ( $\lambda=2.94 \mu\text{m}$ ) and the Er:YSGG ( $\lambda=2.79 \mu\text{m}$ ), have received FDA approval for this purpose and have shown promise for adoption into today's contemporary dental practices. These systems use water within the tooth as the principal absorber as will be discussed below. Subsequently, it was found that these laser systems demonstrated caries preventive effects when used to ablate smooth enamel surfaces[5].

#### **A.2.1.1 Relevant laser physics**

The term "laser" is an acronym for "Light Amplification by Stimulated Emission of Radiation". Photons are the basic units of light and are often thought of as quanta of "particles". Light, x-rays, gamma rays, cosmic rays, microwaves, or radio waves are all examples of quanta of electromagnetic energy. Light can also be thought of as "waves" of electromagnetic energy. Wavelength can be defined as the distance that a photon travels while the electric field completes one oscillation. Light has wavelengths in the visible, ultraviolet, or infrared range of the spectra. The wavelength of electromagnetic energy not only determines its classification but also its physical properties. Current lasers include wavelengths in the range from about 0.1 to  $11\mu\text{m}$ . The shorter the wavelength the more energy it possesses. For example, ultraviolet radiation (shorter wavelength) has more energy than infrared radiation (longer wavelength).

Each laser beam has a distinct three-dimensional spatial profile or "shape". The diameter of the beam, sometimes called the spot size, is needed to calculate the incident fluence,

which is the energy of laser per unit area. This will be explained in greater detail in section B1.2.

A laser beam is generated by directing energy into a medium that amplifies photons and directs them via mirrors, unidirectionally as monochromatic light. This is done by using a photon of exactly the right energy to stimulate an excited electron into a higher energy state. This excited electron then will decay back to a lower energy state, thus releasing stored energy in the form of a second emitted photon. Stimulated emission will occur when the incident photon has exactly the same energy as the released photon resulting in two photons of identical wavelength oscillating in phase together and traveling in the same direction. Each photon can trigger the release of two more photons and the chain reaction process repeats. The goal of stimulated emission is to stimulate the excited atom to emit a photon before the process occurs spontaneously (e.g. spontaneous emission). As each photon that is released is reflected using unidirectional mirrors; one mirror reflecting 100% of the photons to the second mirror which in turn only partially reflects back, say 80% of the photons, thus allowing 20% of the photons to escape. This stimulated emission can either be made continuous or pulsed and results in a focused laser beam of high energy that can be directed into or onto tissues.

The medium that amplifies the photons determine the wavelength of light and include solid crystals, gases, and various liquids[26, 27]. In the erbium systems, the medium is either erbium, yttrium, aluminum, garnet (Er:YAG) or erbium, yttrium, scandium, gallium, garnet (Er:YSGG). In the case of the CO<sub>2</sub> laser, CO<sub>2</sub> gaseous molecules in the

laser chamber are used as the medium to produce infrared radiation in the 9-11  $\mu\text{m}$  wavelength range.

#### **A.2.1.2 Hard tissue optics**

When hard tissues are irradiated the beam can be absorbed, transmitted, reflected or scattered or some combination of these, depending on the optical properties of the particular hard tissue and the wavelength of the laser light used. The tissue response to laser radiation depends on how the laser energy is distributed within the tissue, itself. Absorbed energy is very rapidly (within picoseconds) converted to heat. It is this thermal rise in the tissue that has been thought to be the key to explaining the mechanism of both the ablative[28-37] and the caries preventive effects[1-3, 9-11] of irradiation on hard tissues. Of course, clinically, the thermal rise must be high enough to cause the desired effect but not cause adverse biological effects to the dental pulp[38]. Ideally, laser irradiation effects should be confined at or near the surface zone with little transmission of heat to the pulp. The control of the thermal effects of laser light depend on the wavelength, fluence, and the temporal characteristics of the laser beam (e.g. repetition rate and pulse duration). Each of these variables can be manipulated to ablate dental hard tissue without pathologic heating of the pulp, as will described separately below.

UCSF LIBRARY



### A.2.1.3. Wavelength

Laser light at wavelengths that are strongly absorbed by dental enamel is rapidly converted to heat within a few micrometers of the surface [39-41]. Wavelengths of laser light that are poorly absorbed by enamel will not be useful for ablation or caries preventive effects. At several mid-IR wavelengths ( $\lambda=3-12 \mu\text{m}$ ), scattering is negligible in dental hard tissue and the energy deposition is determined by the absorption coefficient and the tissue reflectance. In this experiment, Er:YAG ( $\lambda=2.94 \mu\text{m}$ ), Er:YSGG ( $\lambda=2.79 \mu\text{m}$ ), and CO<sub>2</sub> lasers ( $\lambda=9.6 \mu\text{m}$ ) were selected because they are all highly absorbed by the dental hard tissue with absorption coefficients of about 795 cm<sup>-1</sup>, 477 cm<sup>-1</sup>, and 8000 cm<sup>-1</sup>, respectively[25, 42]. Fried et al. have shown the principal absorption bands of enamel and the relevant laser wavelengths by analyzing the infrared transmission spectrum of enamel powder (1%) in a KBr pellet [5, 37] (Fig. 1). The Er:YAG at  $\lambda=2.94 \mu\text{m}$  is highly absorbed by the water (H<sub>2</sub>O) between the enamel prisms and around individual crystals[37]. The Er:YSGG at  $\lambda=2.79 \mu\text{m}$  is highly absorbed by both the OH group in dental mineral and the water. The CO<sub>2</sub> at  $\lambda=9.6 \mu\text{m}$  is highly absorbed by the PO<sub>4</sub><sup>3-</sup> groups in dental mineral[25].

UCSF LIBRARY

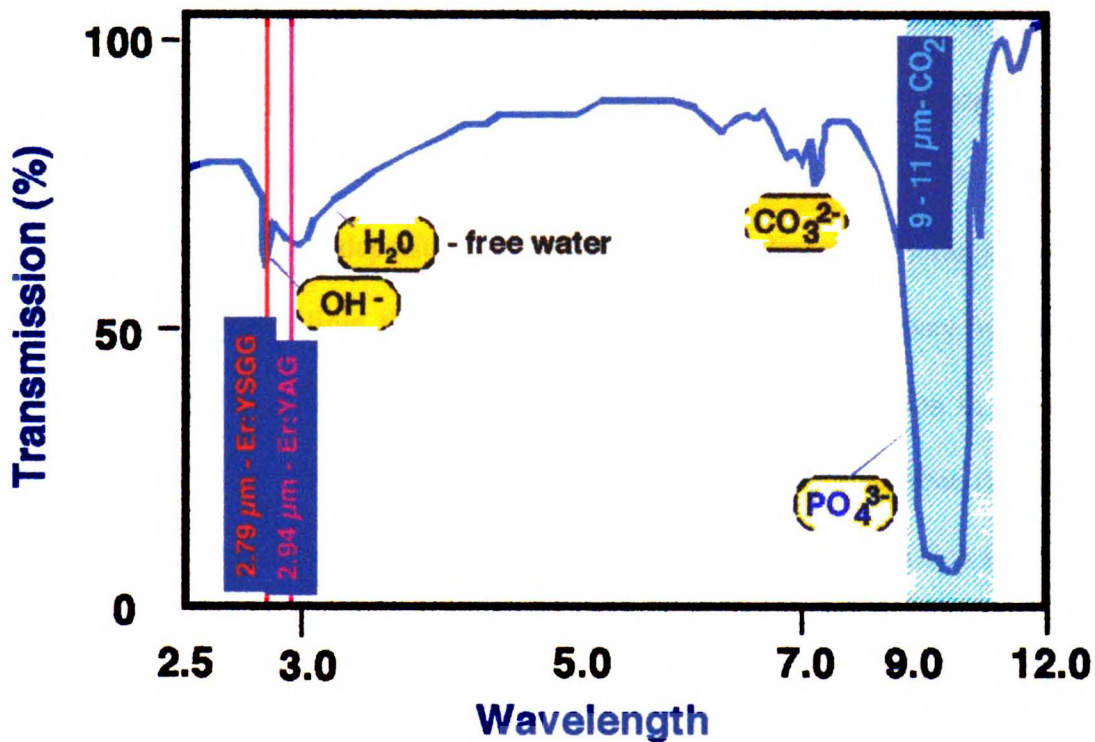
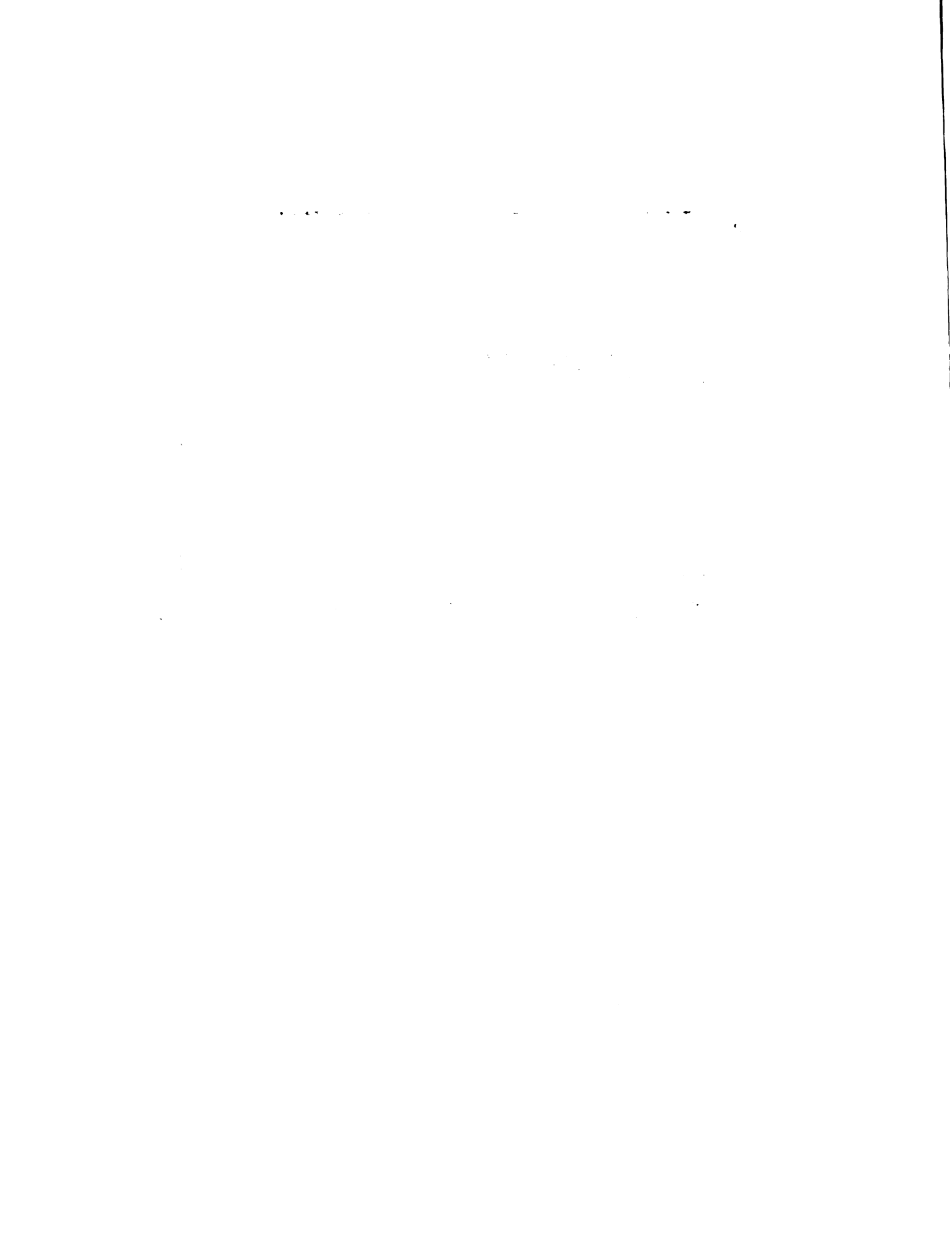


**Figure 1** IR transmission spectrum of carbonated hydroxyapatite (<1%) in a compacted KBr pellet. The laser wavelengths and absorbing species are indicated. The H<sub>2</sub>O corresponds to the OH stretch of water incorporated in the enamel matrix, while the source of the (OH) band is the OH stretch of the carbonated hydroxyapatite mineral. Reproduced with permission from Dan Fried.

Previously reported radiometric surface temperatures at the ablation threshold for enamel indicate that the mechanism of ablation is thermal and occurs at approximately 300-400°C for Er:YAG, 800°C for Er:YSGG, and 1200°C for CO<sub>2</sub> laser irradiation with laser pulses of 100-300 μs duration[37, 39]. Previous studies of caries inhibition on smooth surfaces demonstrated increased resistance to acid dissolution at all the above laser wavelengths[2, 3, 5].

UCSF LIBRARY



#### **A.2.1.4 Pulse Duration**

The amount of time it takes to dissipate approximately half of the energy deposited at the surface zone is called the thermal relaxation time. A pulsed laser with a pulse duration on the order of the thermal relaxation time, allows for short bursts of energy that causes a rapid temperature rise at the surface zone and, although heat does still slowly diffuse, it minimizes the total heat deposition in the deeper layers. For pulse durations longer than the thermal relaxation time, there is sufficient time for heat to flow away from the surface zone at which it is absorbed, leading to excessive heat accumulation in the tooth that could be transmitted to the pulp and cause adverse pulpal effects. Free running erbium laser systems have a pulse duration of approximately 150-250  $\mu\text{s}$ , which is on the order of the thermal relaxation time of dental enamel (which is greater than 100  $\mu\text{s}$ ). The long pulse TEA  $\text{CO}_2$  laser has a pulse duration of 5  $\mu\text{s}$  which is on the order of the thermal relaxation time of dental enamel at 9.6  $\mu\text{m}$ . Previous studies have successfully matched the pulse duration to the thermal relaxation time of enamel using the erbium[5] and  $\text{CO}_2$  laser systems[1]. Therefore, based on these facts and studies, pulse durations of 200  $\mu\text{s}$  for the erbium systems and 5  $\mu\text{s}$  for the  $\text{CO}_2$  laser were selected for the present study.

#### **A.2.1.5 Pulse energy and fluence**

The energy of the laser per unit area is called the incident fluence. It is this energy that creates the thermal effect that is responsible for both the caries inhibitory effects as well as ablation (the mechanisms of both actions are discussed below). At lower fluences that are below the ablation threshold, some IR lasers (those that are highly absorbed by the enamel) have been shown to make the treated surface resistant to acid dissolution[1-3].

At higher fluences, above the ablation threshold, one study showed that Er:YAG ( $\lambda=2.94 \mu\text{m}$ ) and Er:YSGG ( $\lambda=2.79 \mu\text{m}$ ) lasers used to ablate tooth mineral can also demonstrate caries preventive effects (at least on smooth surfaces)[5]. Control of fluence is critical; too low and there will be no caries inhibition effects; too high and you may cause the ablation and/or heat to be excessive (i.e., cut too deep and/or thermally injure the pulp). The thermal effects of the laser ablation of dental hard tissue should create a temperature rise at the surface sufficient to alter the mineral and make it resistant to acid dissolution without causing excessive ablation or undesirable pulpal damage.

#### **A.2.1.6 Repetition rate and number of pulses**

In using pulsed laser systems to ablate dental hard tissue, the time between pulses is critical to allow for cooling so as not to thermally injure the pulp. Thus, although the repetition rate and the number of pulses must be high enough to effectively ablate tooth structure, the repetition rate must also be slow enough to allow for cooling between pulses to avoid excessive heat and pulpal damage.

#### **A.2.1.7 Proposed mechanism of caries inhibition**

Human dental enamel is 85% by volume carbonated hydroxyapatite (CAP) which comprises the mineral component of the tooth. In contrast to pure hydroxyapatite (HA), CAP is contaminated with carbonate that causes defects or imperfections in the enamel crystal. These imperfections are more susceptible to acid dissolution, and these areas are therefore preferentially attacked by the acid during an acid challenge[8]. The remaining 15% by volume is comprised of lipids, protein and water and represents the diffusion

channels through which small molecules such as acids may diffuse into the enamel causing further demineralization of tooth mineral[6, 7]. Previous studies have proposed that heating the surface temperature above 300-600°C will eliminate the carbonate-induced imperfections making the surface more like pure HA and thus more resistant to acid dissolution[1-3, 9-11].

#### **A.2.1.8 Ablation mechanisms**

As mentioned above, tooth mineral has a strong absorption maximum near  $\lambda=2.8 \mu\text{m}$  due to the (OH) in the mineral where the Er:YSGG ( $\lambda=2.79 \mu\text{m}$ ) laser is centered, a broad absorption band centered at  $\lambda=3 \mu\text{m}$  due to the interstitial water around enamel prisms and individual crystals where Er:YAG ( $\lambda=2.94 \mu\text{m}$ ) laser is centered, and the CO<sub>2</sub> laser at  $\lambda=9.6 \mu\text{m}$  is highly absorbed by the PO<sub>4</sub><sup>3-</sup> groups in dental mineral[1]. Although all components of dental hard tissue (mineral, water, protein, and lipid) absorb near  $\lambda=3 \mu\text{m}$ , it is likely water plays the principal role in absorption, and thus ablation, in the case of the erbium laser systems[6, 7]. In enamel, the protein and lipid fraction is proportionally small and is unlikely to have much absorptive effect. It is probable that this organic component will have more of an effect in dentin, cementum, and bone where there is a higher concentration by volume (33%)[37]. Since water is the principal absorber for the erbium systems (and to some extent the OH in the mineral in the case of Er:YSGG), the commonly accepted mechanism of ablation for these laser systems is due to the subsurface expansion or microexplosive effects of water that is responsible for exfoliation or spallation of mineral well below the melting point of enamel (about 1200°C).

WEST LIBRARY

In contrast to the proposed mechanism for the erbium lasers described above, the CO<sub>2</sub> lasers are very highly absorbed by the phosphate mineral component (see Fig. 1 above). The laser energy is absorbed and transformed into heat which essentially vaporizes the mineral above the melting point of CAP (1200°C) causing melting, fusing, and recrystallization of the surface that can be seen by Scanning Electron Microscopy (SEM)[44].

#### **A.2.1.9 Surface temperatures for ablation threshold**

Although the ideal temperature range for inhibitory effects in caries has not yet been established, previous work by Fried et. al. has demonstrated in a laboratory model that ablation was initiated at surface temperatures of approximately 300°C for the Er:YAG laser, and 800°C for the Er:YSGG laser[5]. The same study also demonstrated that significant caries inhibition may occur at irradiation intensities below those temperatures thresholds (e.g., 44% caries inhibition for the Er:YAG laser with an incident fluence of 11.5 J/cm<sup>2</sup> and 60% caries inhibition for the Er:YAG laser with an incident fluence of 12.7 J/cm<sup>2</sup>). Later work by Zuerlein with the CO<sub>2</sub> laser ( $\lambda=9-11 \mu\text{m}$ ) demonstrated surface temperatures greater than 400°C are needed to modify the surface to make it resistant to acid[41,42]. Higher temperatures (in excess of 1200°C) are necessary for CO<sub>2</sub> ablation of tooth structure. This finding is consistent with the different ablation mechanisms mentioned above.

### **A.2.1.10 Peripheral thermal damage**

By manipulation of the laser parameters such as wavelength, fluence, repetition rate, and pulse duration, effective lasers can be designed to ablate dental hard tissue that may generate considerable surface temperatures but cause minimal (less than 3°C) thermal rises in the pulpal tissues[45-47].

### **A2.2 The caries process**

The basic process of dental decay is simple in concept. A bio-film called pellicle, derived from salivary proteins and lipids, is strongly bound to the tooth surface. The pellicle is, in turn, covered by bacteria that comprise the dental plaque[48, 49]. If the bacterial plaque includes sufficient numbers of either mutans streptococci (MS) or lactobacilli (LB), or both, then the by-products of their metabolism will be organic acids, such as formic, lactic, acetic, and propionic acid. Note that MS include several different serotypes of which *S. mutans* and *S. sobrinus* are the principal species found in humans. These acid-producing bacteria (MS and LB) are called acidogenic bacteria. That is, they produce acids when they metabolize fermentable carbohydrates[48-50]. Any fermentable carbohydrate such as glucose, sucrose, fructose, or cooked starch, can be metabolized by these bacteria to produce acid as a by-product of their metabolism[51], dispelling the myth that only “sweets” containing sucrose cause dental caries. The caries process is multi-factorial, involving not only pathogenic factors such as pathogenic organisms (MS and LB) and poor dietary factors but often involves the lack of protective factors such as adequate saliva and the use of topical fluoride. The battle between oral health and dental caries can be thought of as a balance between the pathogenic and the protective factors.



If the pathogenic factors in the oral environment have a greater effect than the natural protective factors, then the acid produced by these organisms will cause demineralization of tooth mineral.

### **A2.2.1 Demineralization**

The organic acids produced by these pathogenic bacteria can dissolve the calcium phosphate mineral of the tooth enamel or dentin, and the process is called demineralization[52-54]. Each time there is fermentable carbohydrate taken into the mouth, it is metabolized by the pathogenic bacteria creating acid. The undissociated acid then diffuses out of the plaque fluid (the fluid between the bacteria in the plaque), through the pellicle covering the tooth and finally into the tooth, itself. Much to the surprise of many, the enamel is actually porous to small molecules such as calcium, phosphate, fluoride and these organic acids. Movement of these small molecules is driven by passive diffusion where molecules travel from an area of high concentration to an area of low concentration. Thus, the diffusion of molecules are said to follow a simple concentration gradient. This diffusion continues until the concentration reaches equilibrium. The organic acids readily diffuse following the concentration gradient into the enamel (or dentin if it is exposed), dissociating to produce hydrogen ions as they travel[53, 55]. The dissociated hydrogen ions then dissolve the mineral releasing calcium and phosphate into solution, which can then diffuse out of the tooth via a similar concentration gradient. The spaces between the enamel crystals that allow these small molecules to diffuse are called diffusion channels. If demineralization is not halted or reversed, the caries lesion progresses and can eventually lead to a cavity or cavitation.

### **A2.2.2 Conventional caries management of the occlusal surface**

A traditional approach to caries management in the US often begins with a careful tooth-by-tooth visual and tactile hard tissue examination. The main detection tools consist of conventional dental radiographs and a sharp dental explorer. The clinicians routinely detect lesions by probing the sharp end of a dental explorer into any suspect areas of the tooth such as white or brown spot lesions, pit and fissures, and marginal discrepancies (e.g., chips or gaps) in existing restorations. Currently, if the sharp explorer “sticks” when pressure is applied to the tip or has “tug back” on withdrawal, then the tactile test is said to be positive for caries. In a paper by Chan in 1993, he noted that this detection technique has not changed much it was first described by Black in 1924[56] and, disappointingly, is still being practiced today. Radiographic detection of caries consist of detecting radiolucent areas on the radiograph that appear consistent with pathology. Once a carious lesion is detected on the radiograph and preferably confirmed by the visual and tactile examination, it will usually be treated with a surgical restorative treatment (often amalgam prepared to a G.V. Black outline form)[16]. Typically treatment will begin with education of the patient and oral hygiene instruction. After the periodontal and restorative treatment is completed, the patient is recalled after a period of time that is usually determined by the periodontal status of the patient. At recall, the patient is again examined, and the process is repeated if other carious lesions are detected.

ULST LIBRARY

### **A2.2.3 Caries Management by Risk Assessment (CAMBRA)**

Caries is an infectious disease that is transmissible to others[57]. Mutans streptococci (MS) and Lactobacilli (LB) are the primary organisms involved in human caries[49] and should be targeted, as would any bacterial infection. It is a multifactoral disease involving not only bacteria but also fermentable dietary carbohydrates, saliva, and the tooth surface, itself. Thus, while traditional methods treat the consequences of infection (e.g., the carious lesions), caries management by risk assessment (CAMBRA) treats those that are at risk by first identifying such individuals, then treating the infection, itself (e.g., the pathogenic bacteria). This is achieved primarily by a chemical rather than a surgical approach, using antimicrobials (0.12% Chlorhexidine Gluconate Oral Rinse) to reduce the number of pathogens and fluoride to enhance remineralization[58], inhibit demineralization[59, 60], and strengthen the enamel surfaces[60]. Dentists no longer need to wait until teeth are damaged in order to begin the treatment of early enamel caries. Thus, CAMBRA is a progressive and positive step towards preventing and curing the disease of dental caries. However, the pits and fissures areas on the tooth present a unique problem because of the very narrow and deep morphology. Most pits and fissures are not cleansible[12], are poorly detected for caries and are not reliably monitored for remineralization, thus remineralization of the occlusal surfaces as a clinical treatment modality is not yet practical. It is not surprising that the proportion of occlusal caries has increased[14]. Since these lesions cannot be presently monitored for remineralization, the first step in restorative procedures should be conservative surgical caries control (temporary or permanent) using conservative preparations when possible,

ULST LIBRARY

along with pit and fissure sealants to eliminate potential niches for pathogenic bacteria to thrive. The deep morphology of the pits and fissures often warrant surgical exploration of areas suspected of having caries such as deeply stained pits or fissures. This surgical exploration, or "caries biopsy" if you will, entails removing the smallest amount of enamel and debris to determine the presence or absence of caries. If caries is found, only the caries is removed, appropriate restorative material is then selected, and the proper preparation done for the selected restorative material. The caries biopsy is traditionally done with a high speed 1/4 round bur, however more recently, lasers and air abrasion have been marketed for this purpose. Both have the advantage of eliminating the noise and vibration of the dental drill and thus present a significant psychological advantage to many patients. While both lasers and air abrasion claim to be able to produce conservative preparations, only the laser technology has the potential to inhibit caries.

### **A.3 Specific Aims**

The overall objective of this study is to determine if specific IR laser irradiation can be used to both ablate and preventively treat the pit and fissure areas of human teeth.

The hypothesis tested in this study was that all three IR lasers, Er:YAG ( $\lambda=2.94 \mu\text{m}$ ), Er:YSGG ( $\lambda=2.79 \mu\text{m}$ ) and CO<sub>2</sub> ( $\lambda=9.6 \mu\text{m}$ ) will effectively ablate pits and fissures and will also show caries preventive effects.

The specific aims of this study were:

1. To carry out *in vitro* experiments to ablate the pits and fissure area of extracted human teeth using Er:YAG ( $\lambda=2.94 \mu\text{m}$ ), Er:YSGG ( $\lambda=2.79 \mu\text{m}$ ), and CO<sub>2</sub> ( $\lambda=9.6 \mu\text{m}$ ) lasers. To accomplish this aim the laser conditions were selected based on the most promising scientific results to date.
2. To determine if, during the ablation process, the enamel surfaces were altered to produce resistance to acid dissolution. To accomplish this aim the following methods were employed: (i) artificial caries like lesions were created following laser treatment using an *in vitro* pH cycling (demineralization/remineralization) model; (ii) thin sections were made perpendicular to the fissure and polarized light microscopy (PLM) was performed to identify representative areas to calculate mineral loss; and (iii) the relative mineral loss, or  $\Delta Z$  values, measured in vol. %  $\times \mu\text{m}$ , were calculated utilizing transverse microradiography (TMR).

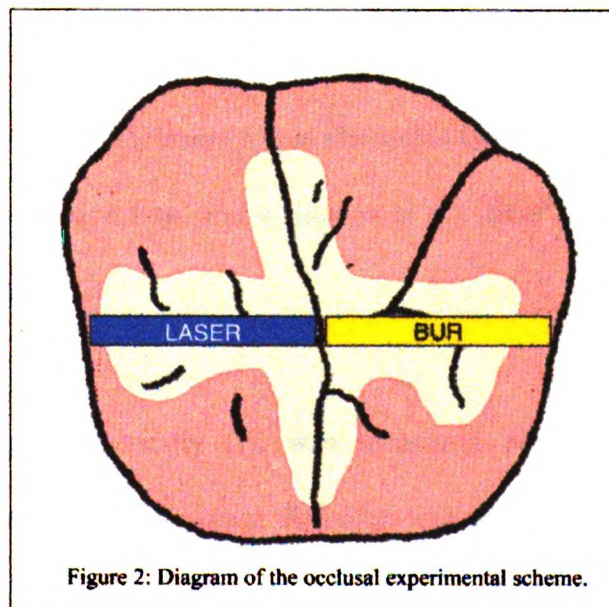
## **B. EXPERIMENTAL DESIGN AND METHODS**

### **B.1. SAMPLE PREPARATION AND LASER ABLATION**

#### **B.1.1 Sample selection and preparation**

Extracted, non-carious and non-restored, permanent human molars were obtained from dentists in the San Francisco Bay Area and were stored immediately in a 0.02% thymol solution. The teeth were then sterilized by gamma radiation using the protocol described by White et al. in 1994[61]. After sterilization, the teeth were inspected visually under a dissecting microscope to eliminate teeth that had any signs of defects, decalcification, or fluorosis in the pit and fissure areas. The crowns with occlusal surfaces that appeared to

be free from obvious caries, with little to no staining of the pits and fissures, were selected and further cleaned by removing any residual soft tissue and brushing with a mild 1% detergent solution and deionized water as previously described by Featherstone et al., 1983. The crowns were sectioned from the roots, in the area of the cemento-enamel junction (CEJ), using a slow speed wet diamond saw after mounting the teeth to a tongue blade with a hot glue gun to stabilize the cut. There were three laser groups, Er:YAG ( $\lambda=2.94 \mu\text{m}$ ), Er:YSGG ( $\lambda=2.79 \mu\text{m}$ ) and  $\text{CO}_2$  ( $\lambda=9.6 \mu\text{m}$ ), with 10 teeth in each group. An occlusal window was created by painting the perimeter of each sample using acid-resistant varnish, approximately 1mm on the outside of the pit and fissure pattern being careful not to allow any varnish to actually get into the pit and fissure so as to interfere with the laser or bur control treatments (Fig 2). The purpose of the acid-resistant varnish was to ensure that only the treated pit and fissure areas were subjected to the artificial caries (e.g., pH cycling) procedures. A total of 30 samples were prepared in this manner.





### **B.1.2 CO<sub>2</sub>, Er:YAG, and Er:YSGG laser ablation**

The laser conditions summarized in Table 1 were selected based on studies discussed in more detail in the previous section titled "Proposed laser systems for caries inhibition and ablation". Since we are evaluating caries prevention during ablation, we selected parameters based on success of previous studies where it was shown that CO<sub>2</sub> lasers at  $\lambda=9.6 \mu\text{m}$  were effective in ablating dental hard tissue[25], and that Er:YAG ( $\lambda=2.94 \mu\text{m}$ ) and the Er:YSGG ( $\lambda=2.79 \mu\text{m}$ ) laser systems have also demonstrated caries preventive effects when used to ablate smooth enamel surfaces[5]. However, because of the deep morphology of the pit and fissure areas compared to smooth surfaces, it was hypothesized (and confirmed by pilot studies) that somewhat higher fluences would be required to more efficiently ablate these areas on human teeth. The hard tissue samples were irradiated with either an Er:YAG ( $\lambda=2.94 \mu\text{m}$ ), Er:YSGG ( $\lambda=2.79 \mu\text{m}$ ) or CO<sub>2</sub> ( $\lambda=9.6 \mu\text{m}$ ) laser. The Er:YAG and Er:YSGG laser was a Schwartz Electro-optics Model 1-2-3 laser using a pulse duration of 200  $\mu\text{s}$  and repetition rate of 2 Hz. The fluence was 64 J/cm<sup>2</sup> for the Er:YAG and 105 J/cm<sup>2</sup> for the Er:YSGG. The CO<sub>2</sub> ( $\lambda=9.6 \mu\text{m}$ ) laser was an Argus STL laser (Argus Photonics Group, Jutpier, FL) with a 5  $\mu\text{s}$  pulse duration, 10 Hz repetition rate, and a fluence of 6.1 J/cm<sup>2</sup>. These laser parameters are summarized in Table 1.

The laser energy, or intensity (I), was measured and calibrated using two laser calorimeters. The spot size, or beam diameter, was measured by scanning a razor blade through the beam. As the razor blade is slowly scanned across the beam it will start to block, or attenuate, the beam. By measuring the intensity (I) at each position of the razor

ULST LIBRARY



blade, we can then plot intensity versus position (the blue line in Figs. 3-5). If we differentiate this resulting curve (the purple line in Figs. 3-5) and fit it to a gaussian distribution (the green line in Figs. 3-5) the beam diameters can be calculated where  $I$  is reduced to  $(1/e^2) = 0.135$ .

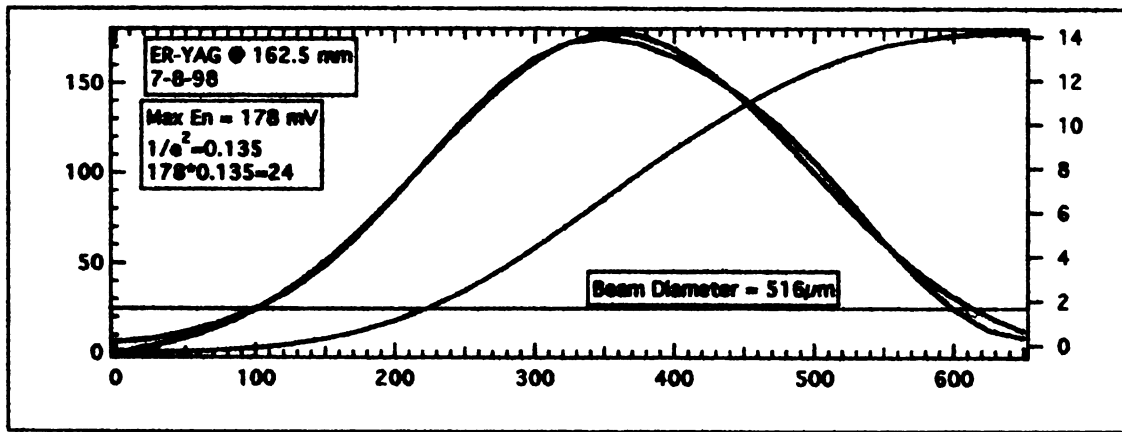


**Figure 3** Er:YAG laser beam profile. The blue line is a plot of the intensity versus position; the purple line is the differential; and the green line is smoothed to a gaussian distribution.

UWF LIBRARY

1. The first part of the document discusses the importance of maintaining accurate records of all transactions and activities. It emphasizes that this is crucial for ensuring transparency and accountability in the organization's operations.

2. The second part of the document outlines the various methods and tools used to collect and analyze data. It highlights the need for a systematic approach to data collection and the importance of using reliable and valid measurement instruments.

3. The third part of the document describes the process of data analysis and interpretation. It discusses the various statistical techniques used to analyze the data and the importance of interpreting the results in the context of the research objectives.

4. The fourth part of the document discusses the importance of reporting the results of the research. It emphasizes that the results should be presented in a clear and concise manner, using appropriate visual aids to enhance the understanding of the findings.

5. The fifth part of the document discusses the importance of drawing conclusions from the research. It emphasizes that the conclusions should be based on the evidence presented in the data and should be supported by logical reasoning.

6. The sixth part of the document discusses the importance of evaluating the research process. It emphasizes that the research process should be evaluated in terms of its effectiveness, efficiency, and reliability, and that the results of the evaluation should be used to improve the quality of the research.

7. The seventh part of the document discusses the importance of disseminating the results of the research. It emphasizes that the results should be shared with the relevant stakeholders and that the research should be used to inform decision-making and policy development.

8. The eighth part of the document discusses the importance of maintaining the integrity of the research. It emphasizes that the research should be conducted in a fair and unbiased manner, and that the results should be reported honestly and accurately.

9. The ninth part of the document discusses the importance of ensuring the ethical treatment of research participants. It emphasizes that the research should be conducted in a way that respects the rights and dignity of the participants and that the results should be used for the benefit of society.

10. The tenth part of the document discusses the importance of ensuring the sustainability of the research. It emphasizes that the research should be conducted in a way that is environmentally friendly and that the results should be used to promote sustainable development.

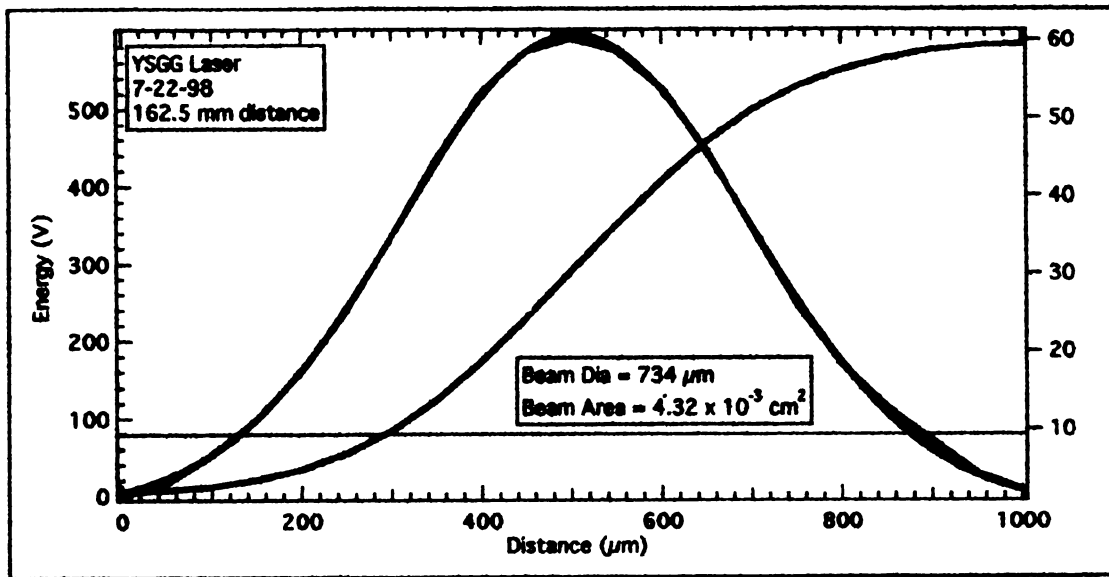


**Figure 4** Er:YSGG laser beam profile. The blue line is a plot of the intensity versus position; the purple line is the differential; and the green line is smoothed fit to a gaussian distribution.

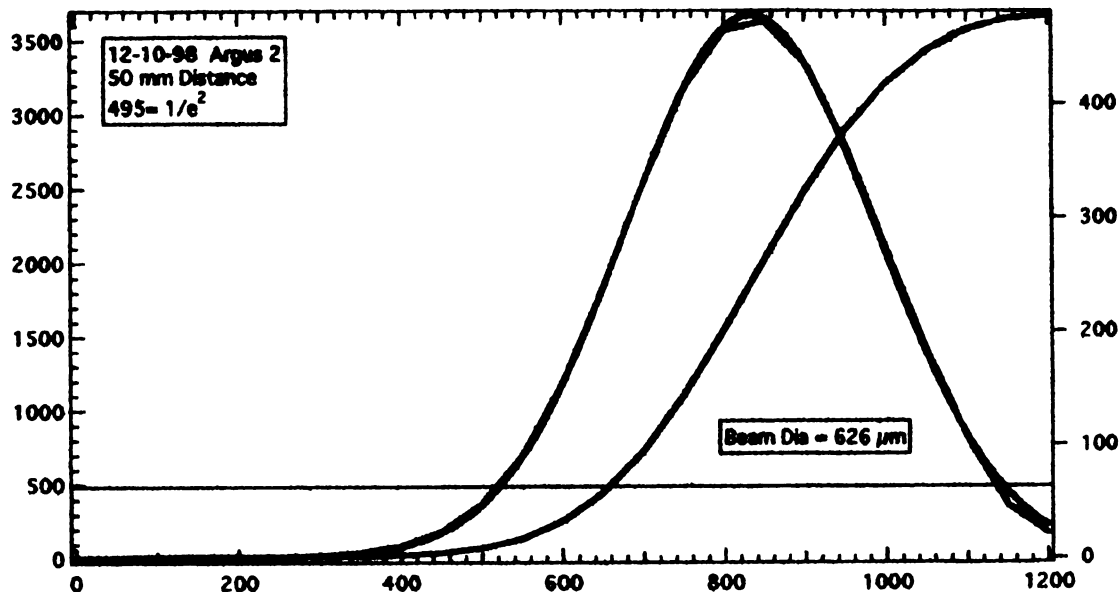
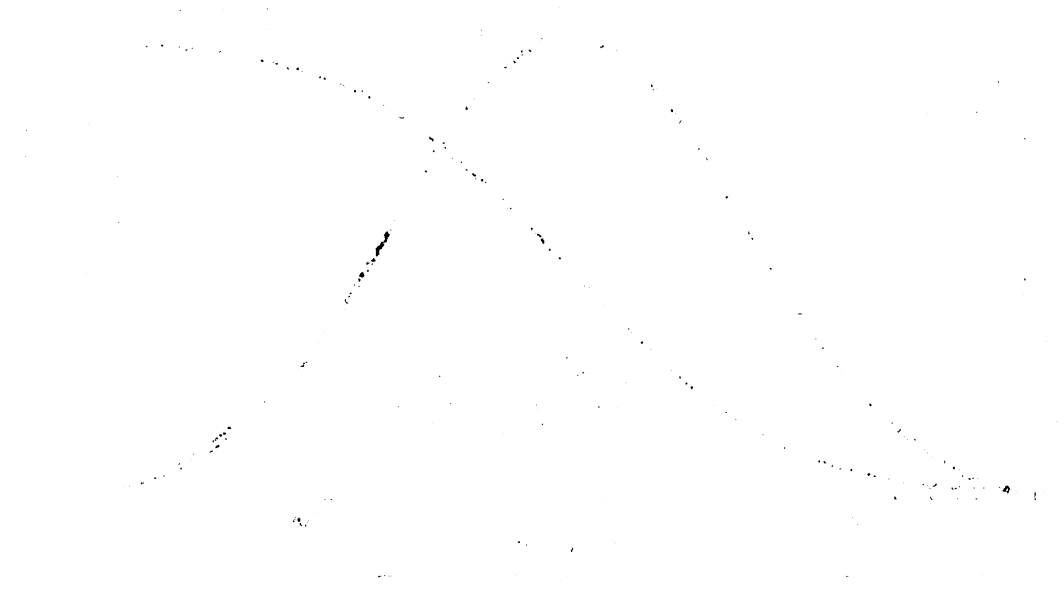


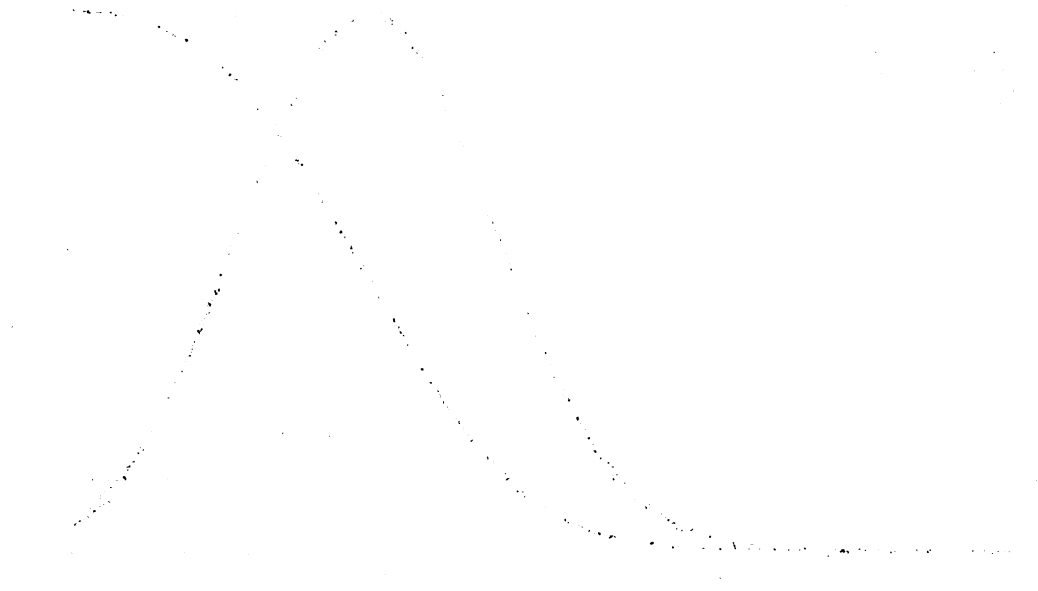
**Figure 5** CO<sub>2</sub> laser beam profile. The blue line is a plot of the intensity versus position; the purple line is the differential; and the green line is smoothed fit to a gaussian distribution.

U.S. LIBRARY

1907 10/10/10



Graph showing the temperature of the water in the bath during the experiment.



Graph showing the temperature of the water in the bath during the experiment.

The beam diameters were 516  $\mu\text{m}$ , 734  $\mu\text{m}$ , and 626  $\mu\text{m}$  for the Er:YAG, Er:YSGG, and  $\text{CO}_2$  irradiation groups, respectively. Once the beam diameters are known, they can be used to calculate incident fluence or energy per pulse measured in Joules (J) per square centimeter ( $\text{cm}^2$ ) of the beam. The incident fluence was found to be 64  $\text{J}/\text{cm}^2$ , 105  $\text{J}/\text{cm}^2$ , and 6.1  $\text{J}/\text{cm}^2$  for the Er:YAG, Er:YSGG, and  $\text{CO}_2$  irradiation groups, respectively. These numbers are summarized below in Table 1 and details of the fluence calculations are seen in Appendix A.

	Er:YAG	Er:YSGG	$\text{CO}_2$
Irradiation Wavelength	( $\lambda=2.94 \mu\text{m}$ )	( $\lambda=2.79 \mu\text{m}$ )	( $\lambda=9.6 \mu\text{m}$ )
Pulse Duration	200 $\mu\text{s}$	200 $\mu\text{s}$	5 $\mu\text{s}$
Number of Pulses per spot	15	15	50
Repetition Rate	2 Hz	2 Hz	10 Hz
Beam Diameter	516 $\mu\text{m}$	734 $\mu\text{m}$	626 $\mu\text{m}$
Energy per pulse	135 mJ	454 mJ	6.1 mJ
Incident Fluence	64 $\text{J}/\text{cm}^2$	105 $\text{J}/\text{cm}^2$	6.1 $\text{J}/\text{cm}^2$

Table 1: Summary of laser parameters used in the present study.

Each of the three lasers were used to ablate approximately one half of the pit and fissure pattern of each of the 10 samples in each test group. The other half of the pit and fissure pattern was used for the bur control. A manually operated digital micrometer stage was used to move the sample approximately 1/3 the beam diameter after each ablation cycle.

ULST LIPK'81

This technique resulted in overlapping of the irradiation areas of each cycle and ensures the entire pit and fissure pattern was ablated without any omissions or gaps.

After ablation of 1/2 the pit and fissure pattern of each sample, the remaining 1/2 of each sample received enamelplasty (e.g., conservative enamel removal) using a 1/4 round carbide bur in a high speed dental handpiece to serve as the bur control as seen previously in Figure 2. It should be noted that no water cooling was used during laser ablation or during the enamelplasty procedures. The reasoning behind this decision will be discussed in the discussion section.

### **B.1.3 Preparation of remineralization and demineralization solutions and their analysis**

Demineralization and remineralization solutions were made according to the pH-cycling model developed by Featherstone and coworkers[2, 3, 62]. The demineralization solution simulates the *in vivo* demineralization process that occurs in the mouth and consists of calcium phosphate (2 mmol/L) in an acetate (0.075 mol/L) buffer. The pH of this solution was adjusted to 4.3.

The remineralization solution approximates the effect of calcium and phosphate from saliva and was described by ten Cate and Duijsters in 1982[63]. The remineralization solution consisted of calcium (1.5 mmol/L), phosphate (0.9 mmol/L), potassium chloride (150 mmol/L) to adjust the ionic strength, and cacodylate (20 mmol/L). The pH of this solution was adjusted to 7.0.

UNIVERSITY OF TORONTO

### **B.1.3.1 Calcium analysis using atomic absorption (AA) spectrophotometer**

A Perkin Elmer 3110 atomic absorption (AA) spectrophotometer was used to measure and validate proper concentration of calcium [Ca] in the demineralization and remineralization solutions. The AA spectrophotometer was first calibrated using standard solutions of 0.5, 1.0, 2.0, 5.0, and 10.0 parts per million (ppm) calcium. These solutions were prepared by diluting a Fisher calcium reference solution containing 1000 ppm calcium with a 1000 ppm KCl solution. Since the AA spectrophotometer requires elemental calcium for the specific wavelength absorption, the presence of potassium plays an important role by suppressing the ionization of calcium in the hot nitrous oxide/acetylene flame.

KCl solution was used to make ten-fold dilution samples of the prepared demineralization and remineralization solutions, then the diluted samples were analyzed using the calibrated AA spectrophotometer. The measured sample values were multiplied by the sample dilution factor to calculate concentration of calcium [Ca] in demineralization and remineralization solutions in ppm. The results are shown in Table 2.

### **B.1.3.2 Phosphate analysis using UV visible spectrophotometer**

A Milton Roy Genesys 5 UV Spectrophotometer was used at a wavelength of 820 nm to measure and validate the proper concentration of phosphate [PO<sub>4</sub>] in the demineralization and remineralization solutions. Phosphate standard solutions of 0, 1, and 2 ppm, and samples of demineralization and remineralization solutions were prepared with Reagent C. Reagent C contains ammonium molybdate that makes a colored complex with

phosphate that absorbs light at 820 nm wavelength[64]. The samples and the phosphate standards were measured in the spectrophotometer. The values were multiplied by the dilution factor, and then divided by mean value of the measured standards to obtain the phosphate concentration [P] (Table 2).

### B.1.3.3 pH calibration

The Tim 900 pH stat machine was calibrated to pH values of 4 and 7 using pH standards from Fisher ChemAlert Guide. Then pH of the demineralization and remineralization solutions were measured and validated (Table 2) before the pH cycling procedure mentioned in B.1.4.

	Actual pH	Expected [Ca] ppm	Actual [Ca] ppm	Expected [P] ppm	Actual [P] ppm
Demin. Soln #1	4.296	80	80.4	62	79.3
Remin. Soln #1	7.0002	60	57.1	29	34.7
Demin. Soln #2	4.296	80	77.7	62	76.3
Remin. Soln #2	6.611	60	60.7	29	37.3

Table 2: Summary of the solution analysis.

### B.1.4 Creating *in vitro* decalcification

After laser ablation in the test groups and enamelplasty in the bur control groups described above in B.1.2, the teeth were subjected for 9 days to an alternating demineralization and remineralizing acid challenge according to the pH-cycling model developed by Featherstone and coworkers[2, 3, 62]. This was done by placing the samples in the demineralization solution for 6 hours, then washing them with double

1:3:2017 JGNN

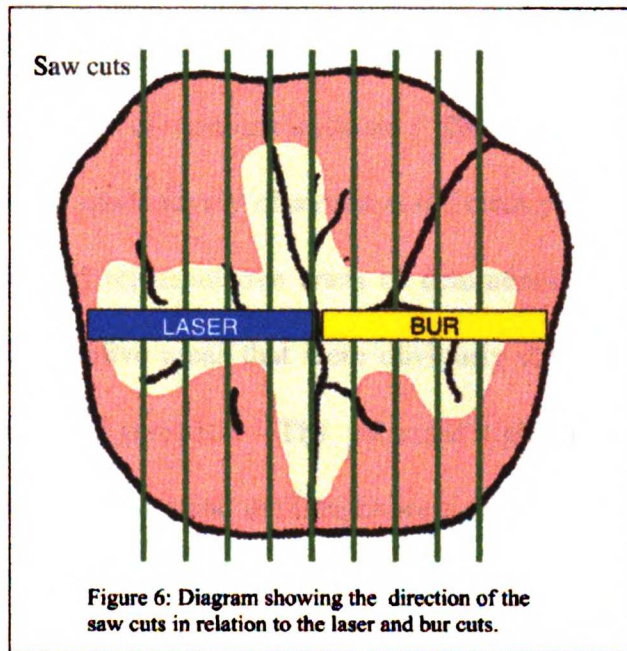


deionized water (DDW) twice and transferring them to the remineralization solution for 17 hours. The samples were stored at 37°C throughout the experiment. This demineralization and remineralization cycling was repeated daily for a total of 9 days. The daily pH-cycling routine was interrupted once because of the weekend and the teeth were stored at 37°C in the remineralizing solution. One hour each day was allowed for manipulation of all the samples before and after demineralization. After the 9 days, teeth were stored in DDW with 0.02% thymol until they were ready for thin sectioning. The pH of the solutions was measured before the 9 days of pH cycling.

#### **B.1.5 Preparation of thin sections using the hard tissue microtome**

At the conclusion of the pH-cycling, each sample was sectioned transversely through the center of the lesions, perpendicular to the fissures (Figure 6). A high speed hard tissue microtome (Scifab, Layayette, CO) with water cooling created approximately 80 µm thin sections.

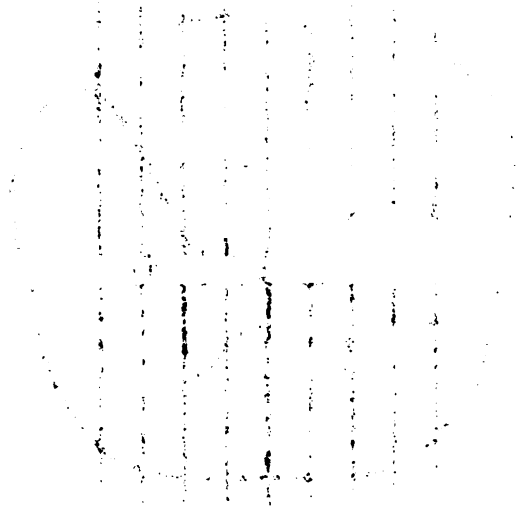
ULM LIBRARY



### B.1.6 Polarized light microscopy

Polarized light microscopy (PLM) was performed, as described in a 1991 review paper by Ten Bosch and Angmar-Mansson[65], on the 80  $\mu\text{m}$  thin specimens (for qualitative purposes only) to visually identify representative areas to measure the relative mineral loss via the Transverse Microradiography (TMR) technique. An Olympus BH3 microscope (using a 530nm filter and a PLM polarizer) coupled with an Optronics DEI-470 imager was used to perform the PLM.

Enamel crystals are birefringent, which means that unpolarized light when entering the enamel crystal will split into two plane-polarized rays (the ordinary and extra-ordinary rays) vibrating at right angles to each other[65]. When the PLM technique is performed on thin 80  $\mu\text{m}$  tooth sections using a polarized light microscope and a U-TP 530



REVISED 1981

polarizing filter, it will transmit only the polarized light enabling the researcher to visually see early areas of demineralization. The changes in birefringence, under magnification, can be qualitatively observed at different positions on the tooth section, making it easy to find representative areas of demineralization and at the same time avoiding non-representative areas that were obviously damaged or chipped during the sectioning procedure (Figure 10). The polarized light images were scanned using BioQuant TCW 3.15 software and the images were printed with the representative areas marked, and sent with the tooth samples to Indiana University where the transverse microradiography was performed. These marked images served as an accurate method to communicate to Indiana University the areas which required the TMR analysis.

#### **B.1.7 Transverse Microradiography (TMR)**

The 80  $\mu\text{m}$  thin sections were coded and sent to Indiana University for TMR analysis. This independent laboratory performed the TMR, and from the images, calculated the relative mineral loss, or  $\Delta Z$  values, measured in vol. %  $\times \mu\text{m}$  on the samples using the Josselin deJong software program via an image analysis system[66-68].

TMR is a quantitative method where the thin transverse tooth section is subjected to mono-chromatic x-rays and microradiograms are made on photographic film. The absorption is compared with the absorption of a simultaneously exposed standard aluminum step wedge[65]. The gray levels on the image are compared with those produced by the step wedge, and volume percent mineral calculated relative to depth

UNIVERSITY OF INDIANA

from the outer surface of this enamel[68]. The computer software mentioned above calculates the area of mineral loss and produces  $\Delta Z$  values, measured in vol. %  $\times \mu\text{m}$ .

### **B.1.8 Statistical analysis**

A power analysis was used to determine the number of teeth in each test group[69]. The power calculations showed that a sample size of 10 in each test group would yield a power of 0.55 with the risk of false positive ( $\alpha=0.05$ ). The ability to detect a 40% change in the enamel was about 65%. One of the ten samples in the YSGG test group and eight of the thirty controls were lost to fracture during thin sectioning.

The  $\Delta Z$  (e.g., relative mineral loss) value for each specimen was calculated from the microradiography profiles. Data from each group was combined to determine mean  $\Delta Z$  and standard deviations were calculated. Single-factor analysis of variance (ANOVA) was performed to identify differences among the four groups. Multiple comparison analysis using the Student-Newman-Keuls test was used to determine differences between the four groups.

#### **B.1.8.1 Deficiencies and errors**

Since the extracted teeth were collected only from the greater San Francisco Bay Area, interpretations extended to the general national or international population should be conservative.

There was some difficulty getting predictable thin sections using the high speed microtome (Scifab, Layayette, CO). Several cuts (3-5 sections) on each sample had to be made in order to get one good 80  $\mu\text{m}$  thin section. Several attempts to find the problem in the cutting procedure did not resolve the problem. Finally, the best explanation for sample fracturing during sectioning was attributed to the deep irregular pit and fissure morphology creating unsupported and unstable enamel walls, and/or the vibration of the saw blade which tended to cause small pieces of enamel to break off. Another observation of this "breaking out effect" during sectioning is the obvious loss of demineralized area on the walls of some bur control samples (Figure 10) causing the base of some of the bur control samples to appear to have more demineralization compared to the walls. After this study was completed, it was discovered that the quality of the saw blades was not to the standard previously experienced and expected. It was discovered, after this study, that changing saw blade manufacturers seemed to eliminate most of the problems experienced in this study.

## C. RESULTS

### C.1 RELATIVE MINERAL LOSS ( $\Delta Z$ ) AND PERCENT INHIBITION

Each of the three laser test groups were irradiated with the laser fluences, pulse number and repetition rate indicated in Table 1 and repeated in Table 3 below. Table 3 also shows the relative mineral loss, or  $\Delta Z$  values (measured in vol. %  $\times \mu\text{m}$ ), standard deviations, and % caries inhibition for each group. The  $\Delta Z$  and (SD) for the control group was 2074(704). The % caries inhibition is defined relative to a control group as  $\{(\Delta Z_{\text{ctrl}} - \Delta Z_{\text{sample}})/\Delta Z_{\text{ctrl}}\} * 100$ . Individual sample data are given in Table 4.

Irradiation Wavelength	Er:YAG ( $\lambda=2.94\mu\text{m}$ )	Er:YSGG ( $\lambda=2.79 \mu\text{m}$ )	CO <sub>2</sub> ( $\lambda=9.6 \mu\text{m}$ )
Pulse Duration ( $\mu\text{s}$ )	200	200	5
Number of Pulses per spot	15	15	50
Repetition Rate (Hz)	2	2	10
Beam Diameter ( $\mu\text{m}$ )	516	734	626
Energy (mJ) per pulse	135	454	19
incident fluence ( $\text{J}/\text{cm}^2$ ) per pulse	64	105	6.1
Mean $\Delta Z$ (vol. % $\times \mu\text{m}$ )	1053	583	1047
Std. Dev.	787	261	416
% Inhibition	50	72	50

Table 3: Summary of results for listed laser parameters

**Delta Z (Mineral Loss [Vol% um])**

Sample Number	Bur Control	YAG Laser	CO <sub>2</sub> Laser	YSGG Laser
1	fractured	1289		
2	1576	1699		
3	2247	247		
4	fractured	894		
5	2736	301		
6	1321	1220		
7	1009	318		
8	fractured	1439		
9	fractured	2707		
10	fractured	419		
11	1581		867	
12	1147		1362	
13	1336		1029	
14	1519		1459	
15	3201		475	
16	3164		1696	
17	3267		1247	
18	Fractured		503	
19	2979		652	
20	3509		1183	
21	3340			222
22	765			773
23	Fractured			1036
24	978			789
25	3337			605
26	1485			583
27	1818			250
28	1922			449
29	1396			538
30	Fractured			Fractured
Mean	2074	1053	1047	583
SD	704	787	416	261
%inhibition	0	49	50	72

**Table 4: Individual sample data. Mineral Loss [Vol% um] values, group mean, SD and % inhibition for each sample**



## C.2 DATA ANALYSIS

The single-factor analysis of variance (ANOVA) indicated that differences existed among the four means at the .01 significance level with an F value of 10.87. Multiple comparison analysis using the Student-Newman-Keuls test showed that all laser test groups were significantly different from the bur control group ( $P < .01$ ), but none of the three laser groups were significantly different from each other. The details of the statistical calculations are shown in Appendix B.

### C.3 POLARIZED LIGHT MICROSCOPY (PLM)

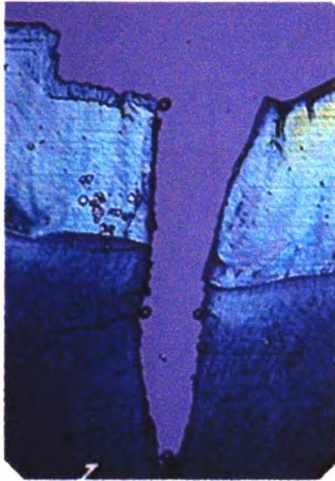


Figure 7 PLM of a sample treated by the YSGG laser

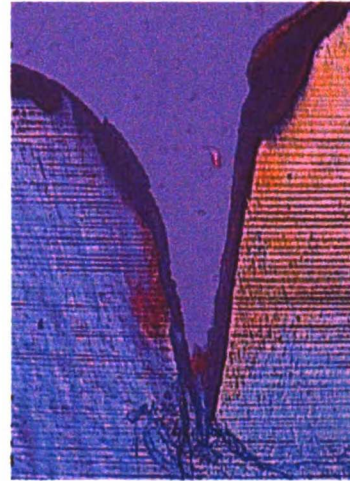


Figure 8 PLM of a sample treated by the CO<sub>2</sub> laser

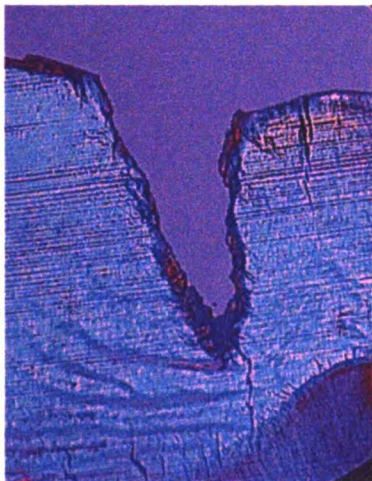


Figure 9 PLM of a sample treated by the YAG laser

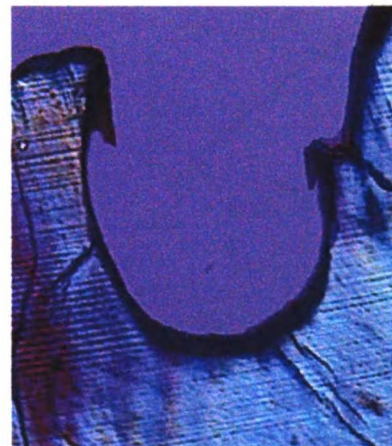


Figure 10 PLM of a Bur control

PLATE I



Fig. 1. *...*

Fig. 2. *...*



Fig. 3. *...*

Fig. 4. *...*

### C.4 TRANSVERSE MICRORADIOGRAPHY (TMR)

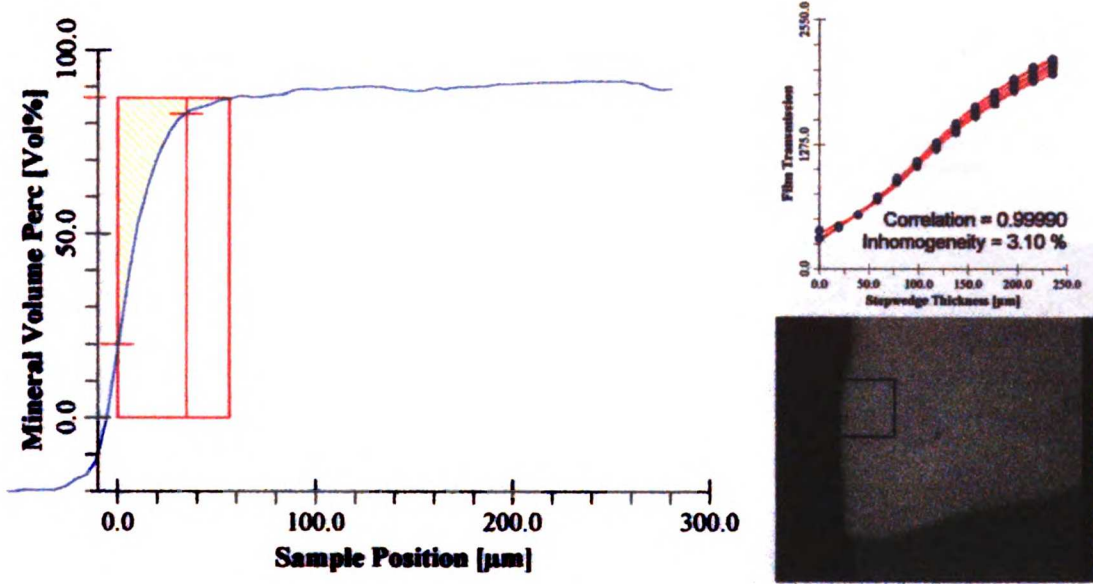


Figure 11: Typical Transverse Microradiography of the YSGG Laser

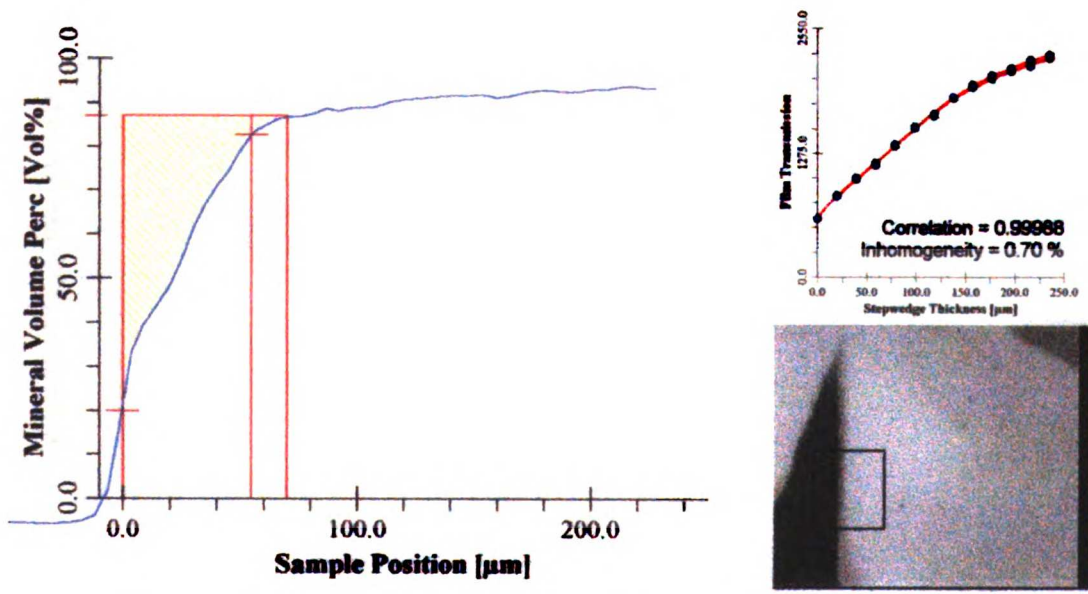


Figure 12: Typical Transverse Microradiography of the CO<sub>2</sub> Laser

1900



1900

1900

1900

1900

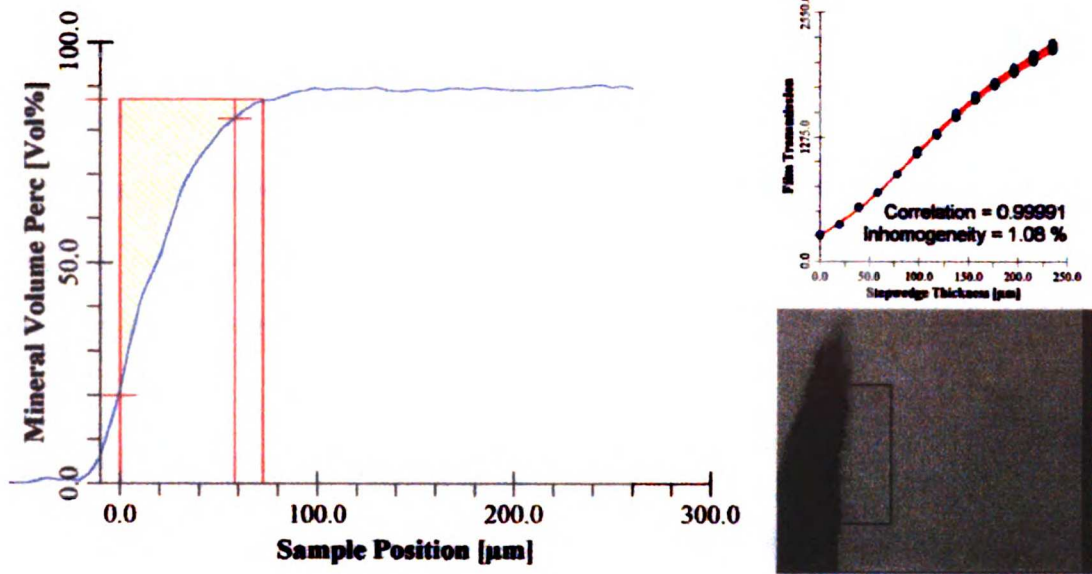


Figure 13: Typical Transverse Microradiography of the YAG Laser

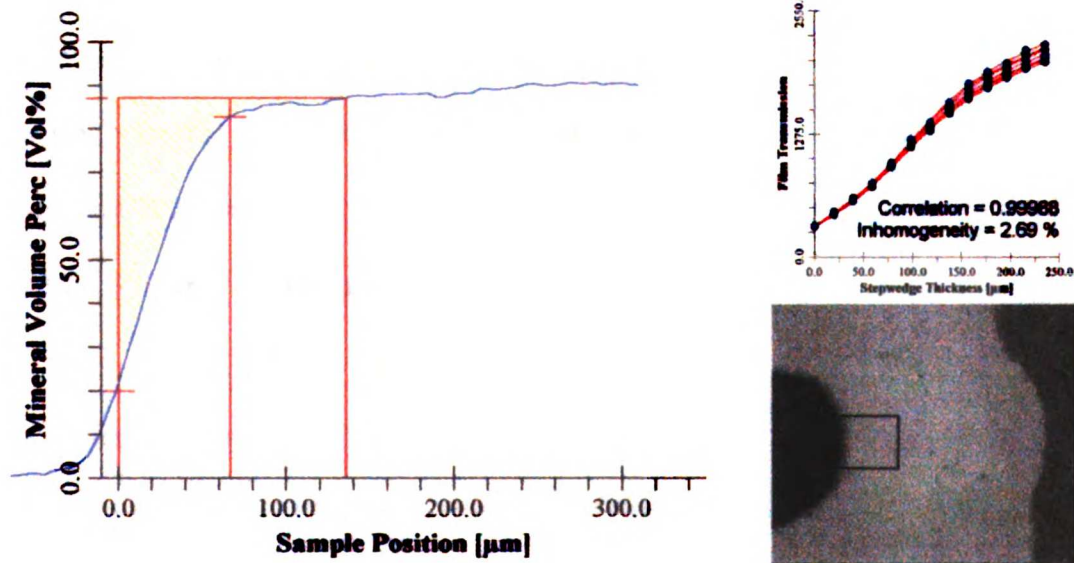


Figure 14: Typical Transverse Microradiography of the Bur Control

APR 19 1951





#### **D. DISCUSSION**

This study demonstrates that the walls of cavity preparations made in occlusal pits and fissures by specific lasers at the irradiation intensities required for efficient ablation of dental enamel using free running Er:YSGG laser (200  $\mu$ s pulse duration), free running Er:YAG laser (200  $\mu$ s pulse duration) and a 9.6  $\mu$ m TEA CO<sub>2</sub> laser (5  $\mu$ s pulse duration), manifest increased resistance to acid dissolution.

Previously reported surface temperatures measured by radiometry at the ablation threshold for enamel indicate that the mechanism of ablation is thermal and occurs at approximately 300–400°C for Er:YAG, 800°C for Er:YSGG and 1200°C for CO<sub>2</sub> laser irradiation with laser pulses of 100–300  $\mu$ s duration[37, 39]. Previous studies of caries inhibition on smooth surfaces demonstrated increased resistance to acid dissolution at all the above laser wavelengths[2, 3, 5] and the % inhibition induced by the laser irradiation scaled with those measured surface temperatures, 44% for Er:YAG at an absorbed fluence (corrected for reflectance losses at surface) of 12 J/cm<sup>2</sup>, 60% for Er:YSGG at 13 J/cm<sup>2</sup>, and 70% for 100  $\mu$ s 9.6  $\mu$ m CO<sub>2</sub> laser pulses at a fluence of 2–3 J/cm<sup>2</sup>, and 49.5% for 5  $\mu$ s, 9.6  $\mu$ m CO<sub>2</sub> laser pulses at 0.75 J/cm<sup>2</sup>[70].

An earlier study by Konishi et al. demonstrated that pulsed CO<sub>2</sub> lasers, namely a 100  $\mu$ s, 9.3  $\mu$ m CO<sub>2</sub> laser, can be used to inhibit dissolution on cavity walls as high as 81%[71]. However, in the Konishi study, the cavity was drilled with a hand piece, and the walls were later irradiated by the laser at 5 J/cm<sup>2</sup>. That fluence was sub-ablative for 100  $\mu$ s – 9.3  $\mu$ m CO<sub>2</sub> laser pulses that require 30 J/cm<sup>2</sup> for efficient ablation of enamel. In this study, the cavity was actually cut by the laser. The 6 J/cm<sup>2</sup> fluence used for the 5- $\mu$ s -



9.6  $\mu\text{m}$  CO<sub>2</sub> laser pulses is actually sufficiently high for the ablation of enamel because of the short pulse duration that is close to the thermal relaxation time for enamel at this wavelength[42].

Currently, clinical adoption of laser technology for cavity preparation using commercially available laser systems has been viewed with some disappointment by those who expect it to do all the functions of a high speed dental drill. One of the major limitations in cavity preparation with the current lasers on the market is that the speed at which the operator can prepare the cavity is much slower when compared to the high speed dental handpiece. Lasers also do not transmit tactile sensation when removing tooth structure which makes it difficult to “feel” caries removal as you would with a dental bur. Lasers are unable to negotiate undercuts and perform precise cuts such as retention grooves, crown or inlay preparations.

However, despite these limitations, the preparation of the pits and fissures for sealants or conservative resin restorations may be well suited for IR laser technology for several reasons. First, the beam diameter of lasers can be made very narrow with the potential to produce very conservative pit and fissure preparations. Of course clinically, methods must be developed to stabilize the laser device when the dentist is preparing the teeth if such narrow preparations are to be realized. A second advantage of using a laser on the pits and fissures is the ability of the laser to not only clean and remove caries but also to create an “etched” surface ready for bonding procedures. Third, as a side effect of peripheral heat deposition during the laser procedure, the walls of the prepared cavity

may acquire an increased resistance to decay. This is of considerable clinical significance and provides a definitive advantage over current technology, because a large percentage of conventional composite restorations will eventually fail due to leakage (especially at the cervical margins)[72] and secondary caries[73]. Neither the dental drill nor the air abrasion units that cut by non-thermal mechanisms have the potential to induce caries preventive effects. A laser demonstrating all these benefits in one procedure without the typical noise and vibration of the dental drill can be viewed as a positive advantage to clinician and patient. For these reasons, many dentist and investigators would consider that to be a significant improvement over the dental drill and air abrasion. At least for now, the clinician must weigh the drawbacks of laser preparation against these unique benefits and discern which is in the best interest of the patient.

IR lasers designed specifically for hard tissues ablate enamel at markedly different temperature thresholds based on whether the principal absorber is water or mineral (Figure 1) The erbium systems (Er:YAG, Er:YSGG) have wavelengths close to the water absorption centered at  $\lambda=3 \mu\text{m}$  and the (OH) group in the tooth mineral with absorption near  $\lambda=2.8 \mu\text{m}$ . It has been proposed that the mechanism of ablation of enamel when using these laser systems is explosive subsurface expansion of water[28-36] (enamel is 8-12% water by volume). Other studies by Fried and co-workers have demonstrated that at  $\lambda=3 \mu\text{m}$ , the water layer on enamel created by water cooling evaporated after the first few laser pulses and did not affect the thermal response of the irradiated tissue. Although water cooling will reduce the risk of thermal damage to the pulp, it should also reduce the

effective ablation rate unless more energy is used to remove the same amount of tissue[37]. The present study was done without any water cooling to first demonstrate that caries preventive effects were possible during ablation of pits and fissures (via thermal effects of ablation). In other words, if water spray was employed initially and no caries inhibition was found, then it would not be known if this negative result was the effect of the water cooling on the laser ablation, itself. Since this study first demonstrated caries preventive effects during ablation without water spray, future studies are now recommended to determine the effect with the inclusion of water cooling.

On a cautionary note, even though the results of this study demonstrated caries preventive effects without water spray, it does not imply that the commercial lasers currently available should be run without water spray in attempts to achieve caries preventive effects. It is possible that the use of water spray for cooling during erbium laser ablation may prevent some, or all, of the caries inhibition effects. Another possible explanation may be that the ablative recoil with water present during the ablation process might remove the modified acid-resistant layer of enamel.

Further caution should be exercised in drawing clinical conclusions from this study regarding fluence. The extremely high fluences employed in this study for ablation with the erbium laser systems may be impractical without the risk of excessive heat accumulation if water spray is not employed. In addition, the high fluences employed in this study for the erbium laser systems may prove to be excessive and unnecessary for highly conservative preparations that do not require high ablation rates. The goal of this

study was not to determine the optimum irradiation conditions that are safe and effective for the preparation of pits and fissures. Future studies need to address parameters that will achieve both optimum safe ablation and caries preventives effects. Also, the higher fluences used in this study by no means imply that higher fluences are better. In fact, studies have shown that hydroxyapatite disproportionates at temperatures exceeding 1500 °C, to form additional calcium phosphate phases that are actually more susceptible to acid dissolution [74]. Therefore, it was a major concern that at very high fluences employed in this study, an abundance of these phases may increase susceptibility to acid. However, that was not the case and the fact that these high fluences did not seem to effect the caries inhibition represents a significant finding.

In summary, the clinical relevance of this *in vitro* experiment demonstrating all three IR lasers could show caries preventive effects during ablation of pits and fissures (without changing laser parameters) and that high fluences did not effect the caries inhibition gives hope that these laser systems have the potential to do this clinically *in vivo*. However, conclusions beyond that should be viewed with caution. Again, the purpose of this study was not to evaluate the best laser parameters and surface temperatures for the clinical ablation of the pits and fissure surfaces. Other laser parameters may alter the ablative efficiency and caries inhibitory effects. Also, none of the lasers used in this experiment used water cooling which may be important clinically. Thus, safe and efficient clinical laser parameters can not be implied by this study. Further, until demonstrated (perhaps by devices or techniques to steady the operator's hand during clinical laser operation), it should not be assumed that the very conservative preparations created by controlled

scanning of the tooth surfaces in the laboratory can be clinically reproducible by the clinician. Thus, future validation of clinical laser systems are necessary. These studies may prove the use of lasers on the occlusal surfaces has the potential to very conservatively clean, etch, and preventatively treat the pit and fissure surfaces all in one procedure.

## **E. REFERENCES**

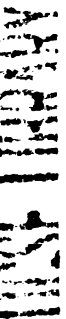
1. Featherstone JDB, Nelson DGA. (1987) Laser effects on dental hard tissue. *Adv. Dent. Res.*, 1, 21-26.
2. Featherstone JDB, Barrett-Vespone NA, Fried D, Kantorowitz Z, Lofthouse J, Seka W. (1995) Rational choice of laser conditions for inhibition of caries progression. Vol. 2394, pp 57-67. SPIE, Bellingham, WA.
3. Featherstone JDB, Barrett-Vespone NA, Fried D, Kantorowitz Z, Seka W. (1998) CO<sub>2</sub> laser inhibition of artificial caries-like lesion progression in dental enamel. *J. Dent. Res.*, 77, 1397-1403.
4. White DJ, Featherstone JDB. (1987) A longitudinal microhardness analysis of fluoride dentifrice effects on lesion progression *in vitro*. *Caries Res.*, 21, 502-512.
5. Fried D, Featherstone JDB, Visuri SR, Walsh JT, Seka W. (1996) The caries inhibition potential of Er:YAG and Er:YSGG laser radiation. Vol. 2672, pp 73-78. SPIE, Bellingham, WA.
6. Curzon MEJ, Featherstone JDB. (1983) Chemical composition of enamel. In: *Handbook of Experimental Aspects of Oral Biochemistry* (ed. EP Lazzari), pp 123-135. CRC Press, Florida.
7. Driessens FCM, Verbeeck RMH. (1990) *Biominerals*. CRC Press, Boca Raton, FL.
8. Featherstone JDB, Silverstone LM. (1985) The Caries Process - Morphological and Chemical Events. In: *Understanding Dental Caries* (ed. G Nikiforuk), pp 261-289. Karger, Basel.
9. Fox JL, Yu D, Otsuka M, Higuchi WI, Wong J, Powell GL. (1992) Initial dissolution rate studies on dental enamel after CO<sub>2</sub> laser irradiation. *J. Dent. Res.*, 71, 1389-1397.
10. Fox JL, Yu D, Otsuka M, Higuchi WI, Wong J, Powell GL. (1992) The combined effects of laser irradiation and chemical inhibitors on the dissolution of dental enamel. *Caries Res.*, 26, 333-339.
11. Fox JL, Wong J, Yu D, Otsuka M, Higuchi WI, Hsu J, Powell GL. (1994) Carbonate apatite as a model for the effect of laser irradiation on human dental enamel. *J. Dent Res.*, 73, 1848-1853.

12. Galil KA, Gwinnett AJ. (1975) Three-dimensional replicas of pits and fissures in human teeth: scanning electron microscopy study. *Arch. Oral Biol.*, 20, 493-495.
13. Kidd EA, Ricketts DN, Pitts NB. (1993) Occlusal caries diagnosis: a changing challenge for clinicians and epidemiologists. *J. Dent.* 21, 323-31.
14. Lussi A. (1991) Validity of diagnostic and treatment decisions of fissure caries. *Caries Res.*, 25, 296-303.
15. Mount GJ, Hume WR. (1998) A new cavity classification. *Austral. Dent. J.*, 43, 153-9.
16. Mount GJ, Hume WR. (1998) *Preservation and Restoration of Tooth Structure*. Mosby.
17. Anusavice KJ. (1998) Chlorhexidine, fluoride varnish, and xylitol chewing gum: underutilized preventive therapies? *Gen. Dent.*, 46, 34-8, 40.
18. Anderson MH, Bales DJ, Omnell K-A. (1993) Modern management of dental caries: the cutting edge is not the dental bur. *J. Amer. Dent. Assoc.*, 124, 37-44.
19. Cooper LF, Myers ML, Nelson DGA, Mowery AS. (1988) Shear strength of composite resin bonded to laser pretreated dentin. *J. Prosth. Dent.*, 60, 45-49.
20. Visuri SR, Gilbert JL, Walsh JT. (1995) Shear test of composite bonded to dentin: Er:YAG laser vs. dental handpiece preparations. *Lasers Dent. (SPIE, San Jose)*, 2394, 223-227.
21. Stern RH, Sognaes RF. (1964) Laser beam effect on hard dental tissues. *J. Dent. Res.*, 43, 873.
22. Stern RH, Sognaes RF, Goodman F. (1966) Laser effect on *in vitro* enamel permeability and solubility. *J. Am. Dent. Assoc.*, 78, 838-843.
23. Ferreira JM, Palamara J, Phakey PP, Rachinger WA, Orams HJ. (1989) Effects of continuous-wave CO<sub>2</sub> laser on the ultrastructure of human dental enamel. *Arch. Oral Biol.*, 34, 551-562.
24. Nelson DGA, Shariati M, Glana R, Shields CP, Featherstone JDB. (1986) Effect of pulsed low energy infrared laser irradiation on artificial caries-like lesion formation. *Caries Res.*, 20, 289-299.
25. Fried D, Zuerlein M, Featherstone JDB, Seka W, Duhn C, McCormack SM. (1998) IR laser ablation of dental enamel: mechanistic dependence on the primary absorber. *Appl. Surface Sci.*, 127-129, 852-856.

APR 1 1951



26. Levy M. (1992) Light, lasers, and beam delivery systems. *Clinics Podi. Med. Surg.*, 9, 521-30.
27. Kutsch VK. (1993) Lasers in dentistry: comparing wavelengths. *JADA*, 124, 49-54.
28. Hibst R, Keller U. (1989) Experimental studies of the application of the Er:YAG laser on dental hard substances: I. Measurement of the ablation rate. *Lasers Surg. Med.*, 9, 338-344.
29. Hibst R, Keller U. (1993) Mechanism of Er:YAG laser induced ablation of dental hard substances. In: *Lasers in orthopedic, dental, and veterinary medicine II*. Vol. 1880, pp 156-162. SPIE.
30. Walsh JT, Deutsch TF. (1989) Er:YAG ablation of tissue: Measurement of ablation rates. *Lasers Surg. Med.*, 9, 327-337.
31. Walsh JT, Jr., Deutsch TF. (1991) Measurement of Er:YAG laser ablation plume dynamics. *Appl. Phys. B*, 52, 217-224.
32. Romano V, Rodriguez R, Altermatt HJ, Frenz M, Weber HP. (1994) Bone microsurgery with IR-lasers: a comparative study of the thermal action at different wavelengths. In: *Laser interaction with hard and soft tissue*. Vol. 2077, pp 87-96. SPIE, Budapest, Hungary.
33. Seka W, Featherstone JDB, Fried D, Visuri SR, Walsh JT. (1996) Laser ablation of dental hard tissue: from explosive ablation to plasma-mediated ablation. Vol. 2672, pp 144-158. SPIE, Bellingham, WA.
34. Izatt JA, Albagli D, Itzkan I, Feld MS. (1990) Pulsed laser ablation of calcified tissue: physical mechanisms and fundamental parameters. In: *Laser-Tissue Interaction*. Vol. 1202, pp 133-140. SPIE.
35. Izatt JA, Sankey ND, Partovi F, Fitzmaurice M, Rava RP, Itzkan I, Feld MS. (1990) Ablation of calcified biological tissue using pulsed hydrogen fluoride laser radiation. *IEEE J. Quant. Electron.*, 26, 2261-2270.
36. Sobol EN. (1995) *Phase Transformations and Ablation in Laser-Treated Solids*. John Wiley & Sons, New York.
37. Fried D, Visuri SR, Featherstone JDB, Seka W, Glana RE, Walsh JT, McCormack SM, Wigdor HA. (1996) Infrared radiometry of dental enamel during Er:YAG and Er:YSGG laser irradiation. *J. Biomed. Optics*, 1, 455-465.



38. Zach L, Cohen G. (1965) Pulp response to externally applied heat. *Oral. Surg. Oral. Med. Oral. Pathol.*, 19, 515-530.
39. Fried D, Seka W, Glana RE, Featherstone JDB. (1996) The thermal response of dental hard tissues to pulsed 9 - 11  $\mu\text{m}$   $\text{CO}_2$  laser irradiation. *Optical Engineering*, 35, 1976-1984.
40. Fried D, Glana RE, Featherstone JDB, Seka W. (1997) Permanent and transient changes in the reflectance of  $\text{CO}_2$  laser irradiated dental hard tissues at 9.3, 9.6, 10.3 and 10.6  $\mu\text{m}$  and at fluences of 1-20  $\text{J}/\text{cm}^2$ . *Lasers Surg. Med.*, 20, 22-31.
41. Zuerlein MJ, Fried D, Seka W, Featherstone JDB. (1998) Modeling thermal emission in dental enamel induced by 9-11  $\mu\text{m}$  laser light. *Applied surface science*, 127-129, 863-868.
42. Zuerlein MJ, Fried D, Featherstone JDB. (1999) Modeling the modification depth of carbon dioxide laser-treated dental enamel. *Lasers in Surgery and Medicine*, 25, 335-347.
43. Featherstone JDB, Fried D, McCormack SM, Seka W. (1996) Effect of pulse duration and repetition rate on  $\text{CO}_2$  laser inhibition of caries progression. *Lasers Dent. II*, 2672, 79-87. SPIE, Bellingham, WA.
44. McCormack SM, Fried D, Featherstone JDB, Glana RE, Seka W. (1995) Scanning electron microscope observations of  $\text{CO}_2$  laser effects on dental enamel. *J. Dent. Res.*, 74, 1702-1708.
45. Arrastia AM, Machida T, al e. (1994) Comparative study of the thermal effects of four semiconductor lasers on the enamel and pulp chamber of a human tooth. *Lasers Surg. Med.*, 15, 382-389.
46. Jennett E, Motamedi M, al e. (1994) Dye-enhanced ablation of enamel by pulsed lasers. *J. Dent. Res.*, 73, 1841-1847.
47. Eder A. (1994) Lasers in dentistry with special reference to internal temperature in the pulp cavity using the excimer laser with 248 nm of different frequencies. *Wiener Klinisch Wochenschrift*, 106, 623-5.
48. Loesche WJ, Hockett RN, Syed SA. (1973) The predominant cultivable flora of tooth surface plaque removed from institutionalized subjects. *Archs. Oral Biol.*, 17, 1311-1325.

APR 1 1971

49. Loesche WJ. (1986) Role of *Streptococcus mutans* in Human Dental Decay. FEMS Microbiol Rev, 50, 353-380.
50. Newbrun E. (1989) Cariology, Third edition. Quintessence Publishing, Chicago, Ill.
51. Geddes DAM. (1975) Acids produced by human dental plaque metabolism in situ. Caries Res., 9, 98-109.
52. Featherstone JDB. (1990) An updated understanding of the mechanism of dental decay and its prevention. Nutrit. Quart., 14, 5-11.
53. Featherstone JDB, Rodgers BE. (1981) The effect of acetic, lactic and other organic acids on the formation of artificial carious lesions. Caries Res., 15, 377-385.
54. Featherstone JDB, Mellberg JR. (1981) Relative rates of progress of artificial carious lesions in bovine, ovine and human enamel. Caries Res., 15, 109-114.
55. Featherstone JDB. (1983) Diffusion phenomena and enamel caries development. In: Cariology Today. Int. Congr., pp 259-268. Karger, Zurich.
56. Chan DC. (1993) Current methods and criteria for caries diagnosis in North America. J. of Dent. Educ., 57, 422-7.
57. Caufield PW, Cutter GR, Dasanayake AP. (1993) Initial acquisition of mutans streptococci by infants: evidence for a discrete window of infectivity. J. Dent. Res., 72, 37-45.
58. Featherstone JDB, Ten Cate JM. (1988) Physicochemical Aspects of Fluoride-enamel Interactions. In: Fluoride in Dentistry (eds. J Ekstrand, O Fejerskov, LM Silverstone), pp 125-149. Munksgaard, Copenhagen.
59. Featherstone JDB, Glana R, Shariati M, Shields CP. (1990) Dependence of *in vitro* demineralization and remineralization of dental enamel on fluoride concentration. J. Dent. Res., 69, 620-625.
60. ten Cate JM, Featherstone JDB. (1991) Mechanistic aspects of the interactions between fluoride and dental enamel. CRC Crit. Rev. Oral Biol., 2, 283-296.
61. White JM, Goodis HE, Marshall SJ, Marshall GW. (1994) Sterilization of teeth by gamma radiation. J. Dent. Res., 73, 1560-7.
62. Featherstone JDB, ten Cate JM, Shariati M, Arends J. (1983) Comparison of artificial caries-like lesions by quantitative microradiography and microhardness profiles. Caries Res., 17, 385-391.



63. ten Cate JM, Duijsters PP. (1982) Alternating demineralization and remineralization of artificial enamel lesions. *Caries Res.*, 16, 201-10.
64. Chen PS, Toribara TY, Warner H. (1956) Microdetermination of phosphorous. *Anal. Chem.*, 28, 1756-1758.
65. ten Bosch JJ, Angmar-Mansson B. (1991) A review of quantitative methods for studies of mineral content of intra-oral incipient caries lesions. *J. Dent. Res.*, 70, 2-14.
66. de Jong EdJ, ten Bosch JJ, Noordmans J. (1987) Optimized microcomputer-guided quantitative microradiography on dental mineralized tissue slices. *Phys. Med. Biol.*, 32, 887-899.
67. de Jong EdJ, van der Linden AHIM, ten Bosch JJ. (1987) Longitudinal microradiography: a non-destructive automated quantitative method to follow mineral changes in mineralized tissue slices. *Phys. Med. Biol.*, 32, 1209-1220.
68. de Jong EdJ, van der Linden AHIM, Borsboom PCF, ten Bosch JJ. (1988) Determination of mineral changes in human dental enamel by longitudinal microradiography and scanning optical mintoring and their correlation with chemical analysis. *Caries Res.*, 22, 153-159.
69. Glanz S. (1992) *Primer of Biostatistics, Third Edition.*
70. Tange T, Fried D, Featherstone JDB. (2000) TEA-CO<sub>2</sub> Laser Inhibition of Artificial Caries-like Lesion Progression in Primary and Permanent Tooth Enamel. *Lasers Dent. VI*, 3910 (eds. P Rechmann, JDB Featherstone, D Fried), pp 306-313. SPIE, Bellingham, WA., San Jose, CA.
71. Konishi N, Fried D, Staninec M, Featherstone JDB. (1999) Artificial caries removal and inhibition of artificial secondary caries by pulsed CO<sub>2</sub> laser irradiation. *Am. J. Dent.*, 12, 213-16.
72. Mjör IA. (1985) Frequency of secondary caries at various anatomical locations. *Oper. Dent.*, 10, 88-92.
73. Kidd EA, Toffenetti F, Mjör IA. (1992) Secondary caries. *International Dental Journal*, 42, 127-38.
74. Featherstone JDB, Fried D, Duhn C. (1998) Surface dissolution kinetics of dental hard tissue irradiated over a fluence range of 1-8 J/cm<sup>2</sup> at a wavelength of 9.3 μm. *Lasers Dent. IV*, 3248, 146-151. SPIE, Bellingham, WA., San Jose, CA.

11/11/11



## **F. APPENDIX**

### **F.1 APPENDIX A: FLUENCE CALCULATIONS**

#### **Er:YAG ( $\lambda=2.94 \mu\text{m}$ , 200 $\mu\text{s}$ pulse duration) LASER**

Given: Beam diameter  $D = 516 \mu\text{m}$

$$\text{Radius (R)} = 258 \mu\text{m} = .258 \text{ cm}$$

$$\text{Volts} = 1.43 \text{ V}$$

$$F = E/A = E/\pi R^2 = 1.43 \text{ V}/(3.14)(.0258 \text{ cm})^2 (10.58 \text{ V/J}) = 64 \text{ J/cm}^2$$

#### **Er:YSGG ( $\lambda=2.79 \mu\text{m}$ , 200 $\mu\text{s}$ pd) LASER**

Given: Beam Diameter = 734  $\mu\text{m}$

$$\text{Radius (R)} = 367 \mu\text{m} = .0367 \text{ cm}$$

$$\text{Volts} = 4.8 \text{ V}$$

$$F = E/A = E/\pi R^2 = 4.8 \text{ V}/(3.14)(.0367 \text{ cm})^2 (10.58 \text{ V/J}) = 105 \text{ J/cm}^2$$

#### **CO<sub>2</sub> ( $\lambda=9.6 \mu\text{m}$ , 5 $\mu\text{s}$ pd) LASER**

Given: Beam Diameter = 626  $\mu\text{m}$

$$R = 313 \mu\text{m} = .313 \text{ cm}$$

$$\text{Volts} = 0.2 \text{ V}$$

$$F = E/A = E/\pi R^2 = E/(3.14)(.313 \text{ cm})^2 = .200 \text{ Volts}/(3.14)(.313)^2 10.58 \text{ V/J} = 6.14 \text{ J/cm}^2$$

## F.2 APPENDIX B: STATISTICAL CALCULATIONS (ANOVA)

	n	x	SD	k =
Control	22	2074.2227	929.3718	4
YAG	10	1053.3900	786.6897	4
CO <sub>2</sub>	10	1047.3600	416.4299	4
Y566	9	582.8778	261.0065	4

$$N = \sum n_i = 22 + 10 + 10 + 9 = 51$$

$$S^2_{\text{within}} = \sum (n_i - 1) S_i^2 = (22-1)(929.3718)^2 + (10-1)(786.6897)^2 \\ + (10-1)(416.4299)^2 + (9-1)(261.0068)^2 = 18,138,370.79 + 5,564,926.157 \\ + 1,560,724.754 + 544,995.1443 = 25,814,016.84$$

$$DF_{\text{within}} = N - K = 51 - 4 = 47$$

$$S^2_{\text{betw}} = \sum n_i \bar{X}_i^2 - (\sum n_i \bar{X}_i)^2 / N = [(22)(2074.2227)^2 + (10)(1053.3900)^2 \\ + (10)(1047.3600)^2 + (9)(582.8778)^2] - [(22)(2074.2227) + (10)(1053.3900)^2 \\ + (10)(1047.36) + (9)(582.8778)]^2 / 51 = [119,776,449.2] - [5,167,640,070 / 51] \\ = [119,776,449.2] - [101,326,275.9] = 17,910,575.90$$

$$DF_{\text{betw}} = K - 1 = 4 - 1 = 3$$

$$DF_{\text{within}} = N - K = 51 - 4 = 47$$

$$F = \frac{S^2_{\text{betw}} / DF_{\text{betw}}}{S^2_{\text{within}} / DF_{\text{within}}}$$

$$F = \frac{17,910,575.90 / 3}{25,814,016.84 / 47} = \frac{5,970,191.967}{549,234,4009} = 10.87$$

$$F_{p < 0.01, 3, 47} = 4.21$$

F is > 4.21 \* Therefore reject the Null hypothesis. There is a difference in at least one of the groups

### F.3 APPENDIX C: STATISTICAL CALCULATIONS (SNK)

	YSGG	CO <sub>2</sub>	YAG	Control
X	582,8778	1047.36	1053.39	2074.2227
n	9	10	10	22

$$S^2_{wit} = \frac{(929.3718)^2 + (786.6897)^2 + (416.4299)^2 + (261.0065)^2}{4}$$

$$S^2_{wit} = 431,037.7205$$

$$DF_{wit} = N - K = 5 - 4 = 47$$

$$q = \frac{(X_A - X_B)\sqrt{2}}{\sqrt{S^2_w/n + S^2_w/n}}$$

$$P = 4 \quad q_{YSGG-cont} = \frac{(2074.22 - 582.88)\sqrt{2}}{\sqrt{\frac{431,037.72}{22} + \frac{431,037.72}{9}}} = \frac{2,109.07}{259.78} = 8.12$$

Since  $q_{YSGG-cont} = 8.12 >$  than  $CRIT_{\alpha,01} = 4.45$  \* Therefore this is **significant** and you should reject the null hypothesis. There is a significant difference.

$$P = 3 \quad q_{YSGG-YAG} = \frac{(1053.39 - 582.88)\sqrt{2}}{\sqrt{\frac{431,037.72}{10} + \frac{431,037.72}{9}}} = \frac{665.40}{301.66} = 2.203 \text{ Not significant}$$

because 2.203 is  $<$   $CRIT_{\alpha,01} = 4.25$

$$P = 2 \quad q_{YSGG-CO_2} = \frac{(1047.36 - 582.88)\sqrt{2}}{\sqrt{\frac{431,037.72}{10} + \frac{431,037.72}{9}}} = \frac{658.87}{301.66} = 2.18 \text{ Not significant}$$

because 2.18 is  $<$   $CRIT_{\alpha,01} = 3.79$

$$P = 3 \quad q_{CO_2 - cont} = \frac{(2074.22 - 1047.36)\sqrt{2}}{\sqrt{\frac{431,037.72}{22} + \frac{431,037.72}{10}}} = \frac{1452.20}{250.39} = 5.8$$

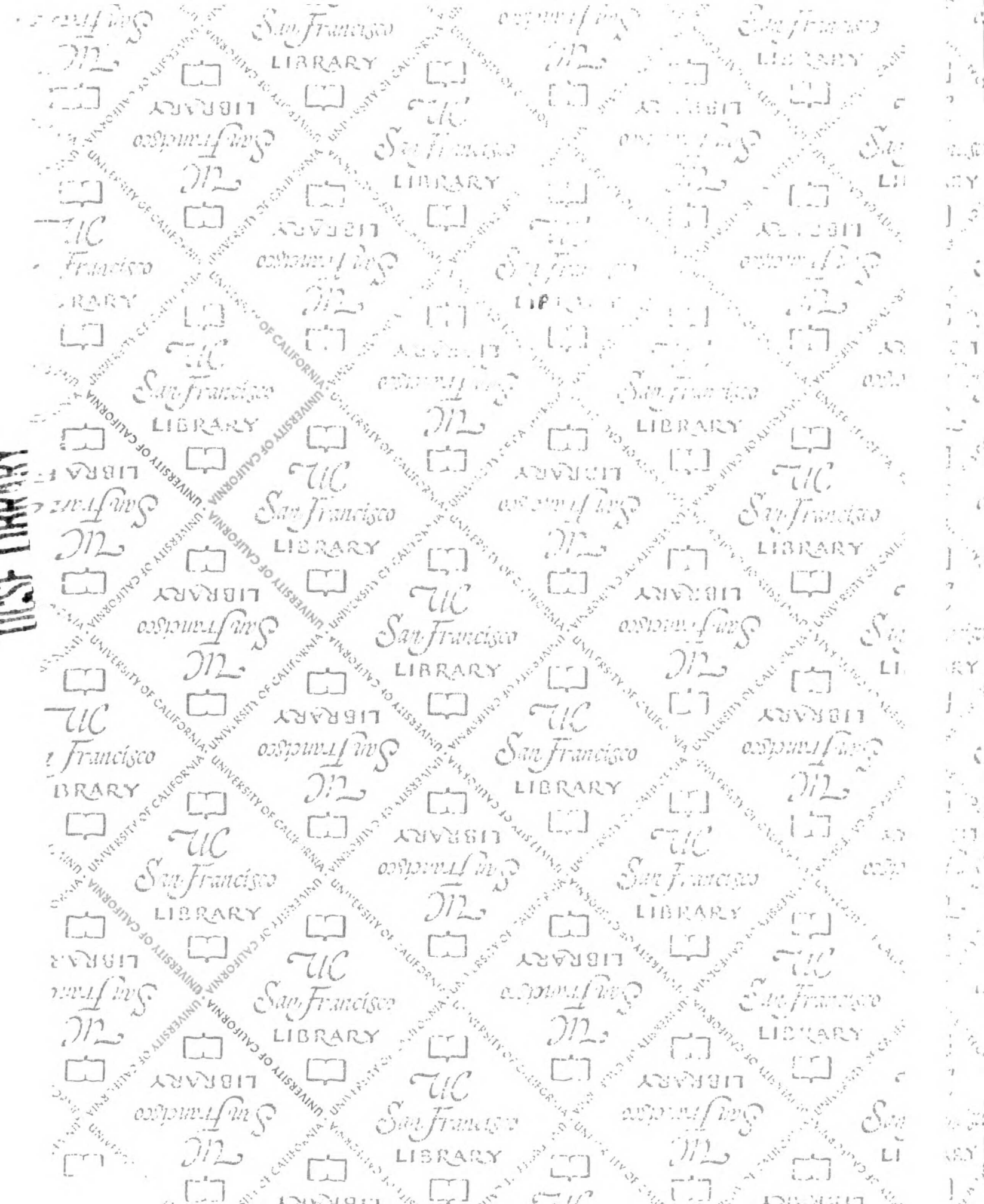
Since  $q_{CO_2\text{-cont}} = 5.8 >$  than  $CRIT_{\alpha,01} = 4.25$  \* Therefore this is significant and you should reject the null hypothesis. There is a significant difference.

$$P = 2 \quad q_{CO_2\text{-cont}} = \frac{(1053.39 - 1047.36)\sqrt{2}}{\sqrt{\frac{431,037.72}{10} + \frac{431,037.72}{10}}} = 0.29 \quad \underline{\text{Not significant}}$$

because  $0.29$  is  $<$   $CRIT_{\alpha,01} = 3.79$

$$P = 2 \quad q_{YAG\text{-cont}} = \frac{(2074.22 - 1053.39)\sqrt{2}}{\sqrt{\frac{431,037.72}{22} + \frac{431,037.72}{10}}} = 5.77$$

Since  $q_{YAG\text{-cont}} = 5.77$  is  $>$  than  $CRIT_{\alpha,01} = 3.79$  \* Therefore this is significant and you should reject the null hypothesis. There is a significant difference.



LIBRARY UNIVERSITY OF CALIFORNIA SAN DIEGO

# For reference

Not to be taken from the room.

6898467



3 1378 00689 8467

LIBRARY

